2022

The Role Of Zooplankton Community Composition In Fecal Pellet Carbon Production In The York River Estuary, Chesapeake Bay

Kristen Nicole Sharpe
William & Mary - Virginia Institute of Marine Science, knsharpe@vims.edu

The Role of Zooplankton Community Composition in Fecal Pellet Carbon Production in the York River Estuary, Chesapeake Bay

A Thesis

Presented to

The Faculty of the School of Marine Science

The College of William & Mary

In Partial Fulfillment

of the Requirements for the Degree of

Master of Science

by

Kristen Nicole Sharpe

January 2022

APPROVAL PAGE

This thesis is submitted in partial fulfillment of

the requirements for the degree of

Master of Science

Kristen Nicole Sharpe

Approved by the Committee, December 2021

Deborah K. Steinberg, Ph.D.
Committee Chair / Advisor

Mark J. Brush, Ph.D.

Carl T. Friedrichs, Ph.D.

Marjorie A.M. Friedrichs, Ph.D.

DEDICATION

This thesis is dedicated to my grandparents – John and Jeannine Drewnowski, and Peter Sharpe Sr. – and my cousin, Corinne Smith – all of whom were always supportive of my dreams, and who I will continue to aspire to make proud.

TABLE OF CONTENTS

ACKNOWLEDGEMENTS

I am eternally grateful for my advisor, Debbie Steinberg, who has served as an outstanding role model for the kind of professional career and personal life I aspire to achieve and has allowed me to pursue my passion in truly incredible places. I am indebted to my committee members – Drs. Mark Brush, Carl Friedrichs, and Marjy Friedrichs – for their kindness as well as their interest, enthusiasm, and support.

Thank you to all members of the Zooplankton Ecology Lab – of which I was privileged to be a part of. An extra special thanks to Joe Cope for sharing his knowledge, support, humor, and questionable taste in music with me; and to Karen Stamieszkin for her guidance in developing, executing, and analyzing my project. To my labmates – Tricia, Jack, Andrew, Tor, Maya, and Claudia – I'm so thankful for your help in the field and lab as well as your friendship and our endless laughter. Thank you to those who helped me out in the lab and field: Schuyler Nardelli, Courtney Lorey, Michael Gibson, and Grace Breitenbeck; and an enormous thank you to Michele Cochran, who was critical in assisting with my CHN analysis lab work!

Thank you to my former coworkers, colleagues, and friends at CBNERR, VIMS, and beyond. A special thank you to Sarah Nuss, Dr. Willy Reay, Sally Lawrence, Celia Cackowski, Lisa Lawrence, Sally Brooks, and Dr. Carol Hopper-Brill for their support in my transition from working life to graduate school.

The VIMS community is exceptional, and I am so grateful for everyone I've had the pleasure of meeting over the past 8 years. A special thank you to Jaclyn McDonald, Sarah Pease, Darryl Trautner, Cassidy Peterson, Zac Chandanais, Lydia Bienlien, Brian Kim, Jackson and Megan Martinez, Derek Detweiler, and Gene Cheung – whose humor, support, encouragement, advice, and love kept me going when I doubted myself.

Finally, there are not enough words to thank my incredible and loving family. My parents and grandparents have always supported my dreams and attending graduate school at VIMS was no exception. My sisters (Darcy and Sarah), brother (David), and brothers-in-law (Chris and El) kept me grounded, sane, and well-fed. My nieces (Caitlyn and Ellie), nephews (Nathan and Colin), and godson (Kenny) continuously give my life meaning and encourage me to keep working to develop the best version of myself. My aunts, uncles, and cousins always cheered me on from afar, and I'm forever grateful for their support.

LIST OF TABLES

LIST OF FIGURES

LIST OF APPENDICES

ABSTRACT

The biological pump is a critical component of carbon transformation in aquatic ecosystems, but the role that zooplankton play in carbon production and vertical export is rarely studied in estuaries. Zooplankton produce carbon-rich fecal pellets which sink to depth and can fuel benthic community metabolism. The body size and taxonomic structure of the zooplankton community varies on interannual, seasonal, and diel time scales, and can lead to varying carbon production and export rates. We quantified fecal pellet carbon (FPC) production by the whole mesozooplankton community (> 200 μm) in the York River, a sub-estuary of Chesapeake Bay. Biomass and taxonomic composition of the near-surface zooplankton community was measured with paired day/night net tows conducted monthly over one year (Jun. 2019 - Nov. 2020). We also conducted live experiments to quantify FPC production rates of both the (size-fractionated) whole community and of dominant individual taxa. Zooplankton biomass generally increased in surface waters at night (2 to 29-fold) due to diel vertical migration. Biomass was low in the winter and high in the summer, with a peak in gelatinous zooplankton biomass in summer the most conspicuous seasonal shift in community composition. *Acartia* spp. copepods were consistently the most abundant taxon, with cladocerans and barnacle nauplii becoming equally abundant in the winter and spring. Whole community FPC production rates were higher (3- to 65-fold) at night than during the day. This was driven by increases in mesozooplankton biomass, especially *Acartia* spp., at night due to diel vertical migration, with the 0.5 – 1 mm size class comprised of *Acartia* spp. contributing 2-26% to FPC production in the day versus 40-70% at night. Daytime FPC production was dominated by the two smallest mesozooplankton size fractions - comprised mostly of *Acartia* and other copepods, barnacle nauplii, rotifers, and cladocerans. Increases in the relative contribution of larger size fractions to total FPC production occurred at night due to diel vertical migration into surface waters of larger animals such as mysids, which produced relatively large and carbon-rich fecal pellets. Seasonal estimates of community FPC production were highest in the fall, intermediate in the spring, and lowest in the summer. Surface FPC production was affected by seasonal shifts in the mesozooplankton community, including increases in the abundance of large migrating animals (mysids, chaetognaths, larval fishes) in the summer and relatively larger calanoid copepods in the fall. Gelatinous zooplankton may have contributed a top-down control limiting community FPC production rates in the summer. This study indicates that zooplankton FPC production in estuaries can surpass that in oceanic systems. Future research on the fate of fecal pellets produced in the surface is needed to understand the role of fecal pellets in vertical carbon export and benthic-pelagic coupling in the York River and other estuaries.

The Role of Zooplankton Community Composition in Fecal Pellet Carbon Production in the York River Estuary, Chesapeake Bay

1. INTRODUCTION

Zooplankton and the biological carbon pump

Zooplankton play a key role in the ocean's biological pump – the biologically-mediated transport of surface community production (i.e., fixed carbon) to depth (Steinberg & Landry, 2017). Zooplankton ingest particulate organic carbon (POC) in the form of phytoplankton, a portion of which is subsequently egested as fecal pellets. Dissolved organic carbon (DOC) is released through sloppy feeding as well as excretion, and leakage of DOC from fecal pellets can further contribute to the DOC pool. Zooplankton fecal pellets passively sinking from surface waters can comprise a large proportion of POC flux to depth (Turner, 2015). Zooplankton that undergo diel vertical migration also actively transport carbon to depth, by grazing in the surface waters at night and migrating to deeper waters where migrators reside during the day and where fecal pellets are egested (Steinberg & Landry, 2017). These zooplankton-mediated export processes support mesopelagic food webs and microbial communities (Anderson & Tang, 2010; Burd et al., 2010; Kelly et al., 2019). The biological pump is also a critical component of pelagic-benthic coupling in aquatic ecosystems, especially in the open ocean where primary production is limited to a shallow depth relative to the extent of the water column (Steinberg & Landry, 2017).

Organic matter that is not consumed and remineralized below the euphotic zone is eventually deposited onto the ocean floor where it can support benthic communities or be buried and effectively sequestered. In estuaries, POC can also be exported out of the estuary through tidal flushing (Pinckney et al., 2001). Cross-system analyses of POC

input and respiration in estuaries indicates that one-quarter of primary production and organic carbon inputs in the surface is respired at the bottom (Nixon, 1981). However, in the open ocean globally, only ~0.1% of surface carbon is deposited onto the seafloor on a time scale of millennia (Berelson, 2001). On an annual basis, marine zooplankton ingest an estimated 9-17 gigatons of carbon and egest fecal pellets containing 6-10 gigatons of carbon (Steinberg & Landry, 2017). Thus, if 0.1% of the carbon in fecal pellets is buried, roughly 6×10^9 kg of carbon is sequestered through pellet-mediated carbon flux per year. It is estimated that carbon dioxide concentrations in the atmosphere would be 50% higher without the biological pump and associated carbon exporting processes (Sanders et al., 2014). Zooplankton thus play a significant role in the global carbon budget, making them a critically important player in climate regulation.

Zooplankton community structure and particle export

The structure of the zooplankton community can affect particle export and lead to differential carbon flux rates in different regions of the ocean (Wilson et al., 2008; Dagg et al., 2014; Stukel et al., 2013; Steinberg & Landry, 2017). Different zooplankton taxa create morphologically distinct fecal pellets with variable carbon content, sinking rates, and likelihood of remineralization versus burial. For example, salps (gelatinous zooplankton) create dense pellets which sink up to 10-fold faster than relatively smaller pellets created by mesozooplankton such as copepods (Turner, 2015).

Zooplankton species composition varies on seasonal and interannual time scales because of changing environmental variables and food availability. Zooplankton can

rapidly respond to environmental changes, particularly temperature (Hessen et al., 2007), leading to an increase in species richness and overall diversity related to increases in water temperature. Seasonal variation in the zooplankton community structure due to temperature can lead to seasonal variation in vertical carbon export. Riser et al. (2010) examined zooplankton fecal pellet contribution to vertical export of particulate organic carbon throughout prominent seasonal changes in a northern Norwegian fjord and found that relative fecal pellet carbon contribution to total POC flux varied seasonally and ranged between 7% during the winter months to 75% during the productive spring season. The authors attributed these high vertical export rates in the spring to increases in the relative abundance of euphausiids, which contributed over 90% of vertical fecal pellet carbon export during the spring.

Zooplankton species composition also varies between day and night due to diel vertical migration, which can affect particle flux. Diel vertical migration is the process whereby zooplankton (and many fishes) ascend from deep water into the surface waters at night to feed and descend again before the sun rises to their daytime residence depth; a behavior that is largely an adaptation for predator avoidance (Hays, 2003; Cohen & Forward Jr., 2009). Diel changes in surface zooplankton community composition in the northeast Pacific Ocean in 2018 led to fecal pellet production rates that were on average double in surface waters at night compared to the day (Stamieszkin et al., 2021).

Understanding changes in zooplankton species composition and the effect on fecal pellet production and vertical export is critical for understanding global carbon flux. While zooplankton fecal pellet production rates have been measured for individual taxa, whole community-level fecal pellet production experiments are rare and include studies

in Norway and the Antarctic polar front (Urban-Rich, 2001), Monterey Bay and coastal California (Dagg et al., 2014), and recently the subarctic Northeast Pacific Ocean (Stamieszkin et al., 2021). As fecal pellet production and subsequent vertical carbon export contributes to carbon sequestration, it is important to expand these community-level experiments to other ecosystems.

Prior estuarine diel vertical migration and fecal pellet production studies

Studies of diel vertical migration have mostly focused on the open ocean (e.g. recently reviewed in Dawidowicz & Pijanowska, 2018) but several have examined estuaries (e.g., Vineetha et al., 2015; Kimmerer et al., 2002; Naylor, 2006; Chew et al., 2015). Few studies of zooplankton diel vertical migration have occurred in the Chesapeake Bay – one specific to cladocerans in the northern Bay (Bosch & Taylor, 1973) and one community-level analysis of two separate regions of the lower Bay (Cuker & Watson, 2002). Cuker & Watson (2002) found that all major zooplankton taxa in Jones Creek migrated from near-bottom waters during the day into surface waters at night. In the James River, larger-bodied and stronger-swimming taxa, including larger size classes of *Acartia tonsa* copepods and mysid shrimps, migrated upward at night, while smaller-sized or early-stage *A. tonsa* and barnacle nauplii underwent a reverse diel vertical migration (Cuker & Watson, 2002). This reverse diel vertical migration was likely a mechanism employed by the smaller animals to avoid predation from larger migrating zooplankton by seeking refuge during the day in the surface waters (Bollens et al., 1992).

Zooplankton fecal pellet production experiments have only been performed in a few estuaries: the Krka Estuary in the Eastern Adriatic Sea (Svensen et al., 2007), the Yangtze Estuary in the East China Sea (Guo et al., 2018), and the Chesapeake Bay (Saba et al., 2011; Stone & Steinberg, 2018). These studies focused on fecal pellet production rates of dominant species only (e.g., copepods, gelatinous zooplankton) and suggest that rates vary on a seasonal basis as well as with estuarine physical and chemical conditions such as circulation, salinity, stratification, and nutrient inputs. For example, a sharp halocline in the Krka estuary concentrates fecal pellets and other organic material at the freshwater-seawater interface which leads to decomposition and coprophagy (consumption of fecal material) and thus low sedimentation rates of fecal pellets (Svensen et al., 2007). Conversely, sediment trap studies and fecal pellet production experiments performed in the Yangtze Estuary show high zooplankton biomass leads to high levels of fecal pellet production and sedimentation, which also varies seasonally (Guo et al., 2018). These studies suggest that rates of fecal pellet production and potential flux in estuaries can rival or surpass rates of fecal pellet export in oceanic systems which have received considerably more attention in this regard. This highlights the need for zooplankton fecal pellet production studies in estuaries such as the Chesapeake Bay where, compared to oceanic systems, diversity of zooplankton is relatively low, but biomass is high (Park & Marshall, 2000) due to high nutrient availability and associated primary production.

The York River estuary

The York River estuary is a major tributary to the Chesapeake Bay, one of the largest estuaries in the world. The York River is characterized by complex physical, chemical, and biological interactions that cause broad variability on a diel, seasonal, and interannual basis. Dynamic, shifting characteristics of the York River influence the zooplankton community through altering the physical environment as well as species composition of phytoplankton and other prey.

Phytoplankton stocks follow a seasonal cycle in the York River, with a pronounced spring bloom following the influx of rainfall into the Pamunkey and Mattaponi rivers (spring freshet) as well as secondary blooms in the late summer caused by increases in water temperature (Reay, 2009). These increases in phytoplankton stock provide increased food availability for higher trophic levels, including zooplankton. During the summer months, the York River experiences periodic bottom hypoxia due to eutrophication and decomposition of algal cells along with increased water column stratification (Lake et al., 2013). Bottom hypoxia can influence the zooplankton community by restricting the use of bottom habitat by planktivorous fishes such as anchovies, thereby creating a type of refuge for zooplankton to avoid predation (Ludsin et al., 2009).

The York River has both a primary and secondary estuarine turbidity maximum where hydrographic parameters and physical processes lead to the resuspension and accumulation of suspended sediment and particulates, including phytoplankton cells. Estuarine turbidity maximum zones and turbidity fronts have been documented to influence spatial distribution and enhance abundance of zooplankton species in various estuarine habitats, including the calanoid copepods *Acartia tonsa* (Derisio et al., 2014)

and *Eurytemora affinis* (Roman et al., 2001). In the Chesapeake Bay mainstem, currents and tides were also found to affect zooplankton biomass, which increased within the mid- to surface water column during maximum flood and ebb tidal current velocities and increased/decreased along with the advance/retreat of the saltwater isocline in that region (Roman et al., 2001).

Objective of this study

The objective of this study was to examine diel and seasonal changes in meso- and macrozooplankton (zooplankton > 200 µm) community composition and associated effects on fecal pellet carbon production in the York River. We quantified both size-fractionated whole community-level and taxon-specific production rates of fecal pellets by the zooplankton community. This study was the first in an estuary to systematically quantify the diel and seasonal production of fecal pellets by the whole zooplankton community, which informed the role of these zooplankton in estuarine carbon cycling and potential vertical flux. Quantifying seasonal changes in carbon production by the zooplankton community also allowed for analysis of how fecal pellet production rates changed with temperature, which can be used in Chesapeake Bay and estuarine carbon cycle modeling.

2. MATERIALS AND METHODS

Zooplankton collection and water quality monitoring

Meso- and macrozooplankton (zooplankton ≥ 200 µm in size) were collected from one mesohaline (37.3224°N, -76.5997°W; depth = 10.4 m) and one polyhaline site (37.2371°N, -76.4019°W; depth = 16.8 m) in the York River estuary (Fig. 1) from June 2019 to November 2020. Paired day/night sampling occurred approximately monthly in the polyhaline site, and once in each of four seasons in the mesohaline site. Diel sampling to quantify changes in zooplankton community structure due to diel vertical migration occurred ~12 hours apart, and consistently during the early flood period of the tidal cycle. This period of the tidal cycle was chosen as a prior study recorded highest surface mesozooplankton abundance during this phase in a similar shallow, temperate estuarine system (Chazarreta et al., 2015).

Zooplankton used for community structure and biomass measurements were collected using a 1-m diameter ring net with 200 µm mesh towed, using an electric winch, off the side of the vessel within the top 2 m of the water column for a duration of 2-5 minutes. One such tow was performed on each cruise, and a General Oceanics mechanical flowmeter was used to measure the volume of water filtered through the net. The sample was immediately split on board, with half poured through nested sieves of 5-, 2-, 1-, 0.5-, and 0.2-mm mesh to produce five size fractions (0.2-0.5 mm, 0.5-1 mm, 1-2 mm, 2-5 mm, and > 5 mm). Each size fraction was rinsed onto pre-weighed 200 µm Nitex disks for biomass measurements. The remaining half-split of the tow was preserved in 4% buffered formaldehyde for later taxonomic identification and enumeration.

Three additional tows with a 1-m diameter ring net (one each with 200 µm, 500 µm, and 1600 µm mesh) were performed to collect live animals to be used in fecal pellet production experiments. The different sizes of mesh were used to exclude smaller

animals in the larger animal size fractions in experiments, and a non-filtering cod end was used to maintain animals in good condition. Live animals were gently released into 20-liter containers filled with whole, unfiltered seawater collected from the same location and transported to shore.

During each cruise, water temperature, salinity, and pH were measured in the surface water using an Apera SX823-B pH/mV/conductivity meter. Light intensity was recorded at both the surface and ~ 0.5 m below surface (Milwaukee MW700 LUX light meter). Water samples for Chlorophyll-a analysis were collected in triplicate from just below the surface, filtered onto Whatman glass microfiber filters, extracted in the dark for 24 hours (Shoaf & Lium, 1976), and analyzed using a 10 AU Turner Design fluorometer. Chlorophyll-a was used as a proxy for food availability for zooplankton in the fecal pellet production experiments.

Zooplankton size-fractionated biomass analysis

Biomass filters were placed in a cooler with an ice pack to keep them cold for transport back to the lab, where they were then placed in a -20°C freezer. For processing, frozen biomass filters were thawed for at least 30 minutes and weighed on a microscale (Sartorius BP211D) to obtain wet weight. Filters were then dried for 24 hours in a drying oven at 60°C, removed, and weighed again to obtain dry weight. Dry weight biomass per cubic meter of each of the five size classes was calculated by dividing biomass measured by the volume of water filtered by the net (mg dry weight m^{-3}).

Zooplankton taxonomic analysis

Taxonomic identification of zooplankton was performed on preserved samples corresponding to days in which community-level fecal pellet production experiments occurred. The sample was first size fractionated through a 1 mm sieve, with all animals >1 mm identified to major taxon and enumerated. The <1 mm size fraction was diluted to 50-100x the total biovolume of animals present, and a 5 mL Stempel pipette was used to collect a subsample, ensuring a minimum of 100 non-*Acartia* spp. (an abundant calanoid copepod) animals were identified and enumerated. Once the identification of non-*Acartia* animals was complete, the <1 mm size fraction was further diluted to 250-500x the original biovolume of animals present, and a 5 mL Stempel pipette was used to collect a subsample for identification and enumeration of *Acartia* spp. copepods. A list of major taxa used in identification can be found in Table 1. Identifications were performed using an Olympus SZX10 stereo microscope at 70-250x magnification.

Fecal pellet production experiments

Both community-level and taxon-specific fecal pellet production experiments were performed, following the methods of Stamieszkin et al. (2021). All experiments were conducted on shore at *in situ* water temperature and light conditions at ~ 0.5-1 m depth using a flow-through incubator covered with light-filtering screen. For community-level experiments, subsamples from the live animal collection tows were live size-fractionated into 5 size classes using nested containers with mesh on the bottom (0.2-0.5 mm, 0.5-1 mm, 1-2 mm, 2-5 mm, >5 mm; corresponding to size-fractionated biomass).

This container was inset into another container with a solid bottom. The animals were thus contained above the inset mesh and separated from their pellets which sank through the mesh and concentrated in the outer container (see Appendix 1 for diagram of the live size-fractionation method; from Stamieszkin et al., 2021).

Each experiment consisted of 12, 4-liter containers: 2 replicates containing animals in each of the 5 size classes in unfiltered (whole) surface seawater, and 2 replicate controls containing whole surface seawater only. The experimental containers were incubated for 4-6 hours, after which the inset containers were lifted – removing the animals – which were rinsed into 15-mL centrifuge tubes and frozen at -20°C. Water from the outer container was then poured through a 56 μm sieve to collect fecal pellets which were rinsed into separate centrifuge tubes and frozen at -20°C.

When processing the samples, the centrifuge tubes were removed from the freezer and thawed at room temperature. Any pellets in tubes containing the animals were first removed, and animals were filtered onto pre-weighed 0.2 mm Nitex disks to be used for dry weight biomass measurements. The pellet fractions were poured into a small, gridded petri dish, photographed, measured (see "Imaging and analysis of fecal pellets" section), and fecal pellet volume was calculated using length and width measurements. Pellets were then filtered onto combusted glass fiber filters and frozen at -20°C prior to particulate organic carbon and nitrogen content (CHN) analysis. Fecal pellet production rates, along with zooplankton biomass data and taxonomic identification, were used to extrapolate production rates within each size class to the whole community (for details see Stamieszkin et al. 2021).

For taxon-specific fecal pellet production experiments, species representative of a large proportion of the zooplankton community collected in each location (including *Acartia* spp. copepods, *Neomysis americana* mysids, and *Livoneca* sp. isopods) were sorted from diluted live tow samples from the bucket by eye, or under a dissecting microscope, counted, and using a wide-bore pipette or spoon gently added to a separate set of 1-liter fecal pellet production experimental jars (Stamieszkin et al. 2021). These jars were also fitted with an inset mesh-bottomed container in which animals were contained, while pellets were concentrated in the outer container. A minimum of 3 replicates including animals in whole surface seawater were prepared for each taxon, along with 3 controls containing whole surface seawater only. Containers were incubated along with the community containers in the flow-through incubator at ambient temperature and light conditions. At the end of the 4-6-hour incubation, the inset containers were lifted – removing the animals – which were either collected with forceps into small centrifuge tubes (mysids and isopods) or rinsed into small petri dishes (*Acartia* spp. copepods) and enumerated under a microscope before being frozen at -20°C. Water from the outer container was poured through a 56 µm sieve to collect fecal pellets and rinsed into separate centrifuges tube which were frozen at -20°C. Upon processing, centrifuge tubes containing the pellet fraction of experiments were removed from the freezer and thawed at room temperature. All pellets were photographed and measured (see "Fecal pellet imaging and carbon to volume conversion" section), and fecal pellet volume was calculated using length and width measurements. Pellets were then concentrated down onto combusted glass fiber filters and frozen at -20°C awaiting CHN analysis. Fecal pellet production rates, along with the number of individual animals in

each experimental jar, were used to calculate production rates per individual within each representative taxon (for details see Stamieszkin et al., 2021).

Fecal pellet elemental analysis

Zooplankton fecal pellets from experiments filtered onto 25 mm combusted glass fiber filters (GFFs) were removed from the freezer and placed in a drying oven at 60°C for a minimum of 24 hours. The filters were then acidifed by fuming with HCl in a dessicator for at least 16 hours to remove inorganic carbon (Gleiber et al., 2012), and again placed in the drying oven for an additional 24 hours before being wrapped in 30 mm tin disks and pelletized. Once pelletized, samples were held in the drying oven at 60°C until they were processed for organic carbon content. CHN analysis was performed using a Costech 4010 Elemental Combustion System.

Fecal pellet imaging and carbon to volume conversion

A calibrated microscope camera system (Olympus SZX 10 stereo dissecting microscope at 25x magnification) was used to image all fecal pellets used in CHN analysis. Measurements (using CellSens software) of pellet length and width were used to calculate fecal pellet volume (assuming a spheroid shape), and fecal pellet carbon content was estimated from carbon to volume relationships determined by our experiments or from the literature. These carbon to volume relationships were also used to calculate pellet carbon content when there was insufficient weight of pellets for a given replicate to detect pellet carbon using CHN analysis (Stamieszkin et al., 2021).

Data analysis

Taxon-specific fecal pellet carbon production rates were calculated by subtracting the average carbon contained in control containers from each experimental replicate, which was then divided by the number of individuals in the replicate as well as the duration of the experiment to calculate a per-individual rate of fecal pellet carbon production (µg C ind^{-1} hr^{-1}). Similarly, for whole community size-fractionated experiments, the average carbon contained in control containers was subtracted from each experimental replicate (each of the size-class containers was treated as a replicate). Mean fecal pellet production rates were calculated using carbon content of pellets produced per dry weight of organisms in each of the five size fractions (mg C $mgDW^{-1}$ hr^{-1}) and were averaged between replicates (n=2) within each experiment. Calculated fecal pellet production rates were applied to measurements of size-fractionated mesozooplankton biomass (mg DW m^{-3}) and summed to determine whole community fecal pellet production rates (mg C m^{-3} hr^{-1}).

3. RESULTS

3.1 Environmental setting

Surface water temperatures were similar between the two sites, ranging from 8.3 – 30°C at the polyhaline site and 9.3 – 30.4°C at the mesohaline site (Fig. 2a). Temperatures followed a typical seasonal pattern, being lowest in February and increasing to a maximum in July (Fig. 2a). Surface water salinity was typically around 5 units lower in the mesohaline site than the polyhaline site and ranged from 5-19

(mesohaline) and 11-24 (polyhaline) (Fig. 2b). Salinity dropped to a minimum in both sites in November 2020 due to a sustained, 3-day heavy rain event prior to sampling. Chlorophyll-a concentrations varied considerably in both sites, with a range of 2.2 – 16.9 μg L^{-1} in the polyhaline site and 3.9 – 20.5 μg L^{-1} in the mesohaline site (Fig. 2c). Chlorophyll-a was usually higher in the mesohaline site, consistent with previous studies reporting relatively higher chlorophyll-a concentrations in the mesohaline York River.

3.2 Diel and seasonal trends in zooplankton biomass and size structure

In the polyhaline site, zooplankton biomass increased in the surface waters at night 2- to 29-fold due to diel vertical migration, except for Nov. 2019 in which biomass decreased in the surface waters at night (Fig. 3a). The size structure of the community also shifted from day to night, with an increase in biomass of intermediate and larger size classes (0.5 – 1 mm, 1 – 2 mm, and 2 – 5 mm) in surface waters at night. Total zooplankton community biomass (mg DW m^{-3}) was lowest in April and increased to maximum values in August of each year (Fig. 3a). Gelatinous zooplankton biomass was high and peaked in the summer months in 2020 due to the presence of large scyphozoan medusae (see section 3.3.2) but was lower in the summer of 2019. In the mesohaline site, biomass – especially of the intermediate and large size classes – also generally increased in the surface waters at night (with exception of Aug. 2019) (Fig. 3b). Although mesohaline sampling was more limited, total community biomass was comparable to the polyhaline site, and high gelatinous zooplankton biomass was present in summer of both 2019 and 2020 (Fig. 3b).

3.3 Diel and seasonal trends in zooplankton abundance and community composition

3.3.1 Diel vertical migration in the polyhaline site

Of the 18 major zooplankton taxa identified in the samples, 15 had higher mean density in surface waters at night than during the day, with two groups (*Acartia* spp. copepods and isopods) exhibiting significant ($p < 0.05$) diel vertical migration, and five (phoronids, chaetognaths, other calanoid copepods, mysids, and larval fishes) exhibiting strong, but not statistically significant ($0.05 < p < 0.10$) diel vertical migration (Fig. 4). Three taxa (barnacle larvae, cladocera, and ctenophores) had lower mean density in the surface waters at night than during the day, but these differences were not significant ($p > 0.05$). Among the taxa with higher mean density at night than during the day, mean night:day (N:D) abundance ratios ranged from 1.75 for decapods to 44.5 for chaetognaths. In addition to chaetognaths, the strongest vertical migrators included teleosts (mean N:D = 13.6), non-*Acartia* spp. calanoid copepods (11.9), annelids (9.6), and phoronids (8.6). N:D ratios could not be calculated for harpacticoid copepods, mysids, or scyphozoans, as they were either only present at night (harpacticoids and mysids) or otherwise did not have any paired monthly day and night abundances (scyphozoans).

3.3.2 Seasonal trends in taxa abundance and community composition

In both the polyhaline and mesohaline sites, *Acartia* spp. copepods were the most abundant taxon, with abundances of 1.5-31 x 10^3 individuals m^{-3} in the polyhaline and

10-44 x 10^3 individuals m^{-3} in the mesohaline site. In the polyhaline site, densities of most copepod groups (including *Acartia* spp., non-*Acartia* calanoids, and cyclopoids) were highest in Sept. 2020 (Fig. 5; Appendix 2), while harpacticoids were present only in Mar. 2020 at night (Appendix 2). In the mesohaline site, daytime densities of *Acartia* spp., other calanoids, and cyclopoids were higher in Feb. 2020 than Nov. 2019 (Fig. 6, Appendix 3a), while *Acartia* spp. densities increased in Nov 2019 at night due to diel vertical migration (Fig. 6). Siphonostomatoids were present only during the day in Nov. 2019 (Appendix 3a).

The second- and third-most abundant taxa (after *Acartia* spp. copepods) were Cladocera and Balanidae. Cladocera (including two species, *Podon polyphemoides* and *Evadne nordmanii*) and barnacle (*Balanus* sp.) nauplii and cyprids were most abundant in Feb. and Mar. 2020 in both the polyhaline (Fig. 5) and mesohaline (Fig. 6) sites and occurred in low densities the rest of the year. Mysids and isopods occurred in both sites, with highest densities in the summer and fall at night and lower densities the rest of the year (Fig. 5). Decapod (primarily crab zoea) densities were higher in the polyhaline site (Fig. 5) than the mesohaline site (Fig. 6), with a peak in summer. Mollusks, chaetognaths, and annelids were present in both sites, with mollusks and chaetognaths being most abundant in the summer and fall and annelids in the spring through summer (Fig. 7, Appendix 3b). Other taxa found only in the polyhaline site included phoronid (horseshoe worm) larvae, larvaceans, and larval fishes – which were most abundant in the summer and fall at night (Fig. 7).

The most abundant gelatinous zooplankton in both sites were hydrozoan medusae, primarily *Nemopsis bachei*, which were present throughout the spring and summer (Fig.

8a, b). Ctenophores (*Beroë ovata* and *Mnemiopsis leidyii*) were most abundant in both sites in Nov. 2019, but also in late summer 2020 in the polyhaline site (Fig. 8a). Scyphozoan medusae (including *Chrysaora chesapeakei, Cyanea capillata,* and *Aurelia aurita*) occurred in Nov. 2019 (day) and Aug. 2020 (night) in the polyhaline site (Fig. 8a), and in Feb. 2020 (day) in the mesohaline site (Fig. 8b), which caused peaks in gelatinous zooplankton biomass (Fig. 4).

3.4 Fecal pellet production experiments

3.4.1 Taxon-specific fecal pellet production

Due to diel changes in abundance, individual taxon-specific fecal pellet production experiments with *Acartia* spp. were performed during both day and night while experiments with mysids and isopods were performed only at night (Table 2). Isopods (*Livoneca redmanii*) had the lowest mean fecal pellet volume (4.8×10^{-4} mm^3), *Acartia* spp. pellets were intermediate (1.25×10^{-3} mm^3), and mysids (*Neomysis americana*) had the highest mean fecal pellet volume (3.0×10^{-3} mm^3). The mean weight of carbon per fecal pellet was highest in isopods (0.67 µg C pellet^{-1}), followed by mysids (0.52 µg C pellet^{-1}), and lowest for *Acartia* spp (0.29 µg C pellet^{-1}). Mean fecal pellet carbon to biovolume ratios were highest for isopods (1.21 mg C mm^{-3}), followed by *Acartia* spp. (0.55 mg C mm^{-3}), and were lowest for mysids (0.42 mg C mm^{-3}) (Table 2).

Acartia spp. individual fecal pellet carbon (FPC) production rates (0.01-0.07 µg C ind^{-1} hr^{-1}) were significantly lower than those of both mysids (0.34-0.51 µg C ind^{-1} hr^{-1}) and isopods (0.19-0.29 µg C ind^{-1} hr^{-1}) (one-way ANOVA, $p < 0.05$), while rates were not significantly different between mysids and isopods (paired sample t-test, $p > 0.05$).

Conversely, weight-specific FPC production was highest in *Acartia* spp. (3.48-4.22 µg C $mgDW^{-1}$ hr^{-1}), followed by mysids (0.19-0.70 µg C $mgDW^{-1}$ hr^{-1}), and lowest for isopods (0.005-0.011 µg C $mgDW^{-1}$ hr^{-1}) (Table 2). *Acartia* spp. individual FPC production rates were highest in Sept. and Nov. 2020 (Fig. 9). There was no significant difference in *Acartia* spp. individual FPC production rates between the day and night (paired sample t-test, $p > 0.05$).

3.4.2 Community-level fecal pellet production

Weight-specific FPC production rates (mg C $mgDW^{-1}$ hr^{-1}) were calculated for each size class in each experiment, and then averaged across all experiments to provide average rates per size class. There was no significant difference in weight-specific rates between the sites (one-way ANOVA, $p > 0.05$), thus results from mesohaline and polyhaline experiments were combined to calculate overall average rates of production per size class (Fig. 10). Generally, fecal pellet volume increased with increasing size class (Table 3), but the differences were not significant (one-way ANOVA, $p > 0.05$). Volume-specific FPC content was not significantly different between size classes (one-way ANOVA, $p > 0.05$). Overall mean weight-specific FPC production rates per size class were not significantly different (one-way ANOVA, $p > 0.05$).

While weight-specific FPC production rates were not statistically different between size classes, when weight-specific rates were applied to biomass measurements to calculate whole-community FPC production (mg C m^{-3} hr^{-1}), there was a significant difference in mean FPC production rates among size classes as well as between day and night in the polyhaline site (one-way ANOVA, $p < 0.05$ for both). Whole-community

FPC production rates were highest in the two smallest size classes in both sites (Figs. 11 and 12). Daytime FPC production was highest in Nov. 2019 in the polyhaline site (Fig. 11), and in Feb. 2020 in the mesohaline site (Fig. 12). Nighttime FPC production in the polyhaline site was lowest in Sept. 2020 (Fig. 11).

In the polyhaline site, the smallest size class (0.2 – 0.5 mm) dominated daytime FPC production across seasons – contributing 62-96% of community FPC production (Fig. 11b). There was a higher contribution of larger size classes to total FPC production at night, with the 0.5 – 1 mm size class contributing 40-70% of total FPC production at night versus 2-26% during the day (Fig. 11b). In the mesohaline site, there was a large increase in daytime FPC production from Nov. 2019 to Feb. 2020 (Fig. 12a) along with an increased relative contribution of the largest size class (> 5 mm) to total FPC production from 4% to 26%, respectively (Fig. 12b). Overall, hourly community FPC production rates in the polyhaline site were higher at night (mean: 18.7 ± 2.09 mg C m^{-3} hr^{-1}) than during the day (mean: 7.2 ± 3.85 mg C m^{-3} hr^{-1}) (Fig. 13a), driven by increases in biomass at night due to diel vertical migration (Fig. 13b).

4. DISCUSSION

Diel and seasonal trends in zooplankton community structure

Of the 18 major taxa identified in samples, 15 had higher mean density in surface waters at night than during the day. *Acartia* spp. had significantly higher densities in the surface at night, consistent with previous studies of diel vertical migration in Chesapeake Bay tributaries (Cuker & Watson, 2002) and other regions (Bollens et al., 1992; Holliland

et al., 2012). Additional strong migrators included chaetognaths, larval fishes, and non-*Acartia spp.* calanoid copepods. Larval fishes (e.g., *Anchoa mitchilli*) may benefit from diel vertical migration through up-estuary transport and retention of larvae in areas of high food abundance (North & Houde, 2004). Chaetognaths (*Sagitta* spp.) vertically migrate in a variety of ecosystems (Kehayias & Kourouvakalis, 2010; Parra et al., 2019), matching vertical distribution with that of their prey (copepods, larval fishes, and decapods) (Kehayias & Ntakou, 2008; Steinberg & Condon, 2009). Mysids, which were generally only observed at night, are strong diel vertical migrators in the Chesapeake Bay and other estuaries (Cuker & Watson, 2002; Calliari et al., 2001) and are disproportionately important in the diets of zooplanktivorous and juvenile demersal fishes in Chesapeake Bay (Sweetman, 2018). Barnacle nauplii and cladocerans (predominately *Podon polyphemoides*) were more abundant in surface waters during the day than at night, displaying patterns of reverse diel vertical migration consistent with previous studies (Cuker & Watson, 2002; Valentin et al., 2003; Bosch & Taylor, 1973). Reverse diel vertical migration reduces predation pressure and resource competition with larger upward-migrating zooplankton (Bollens et al., 1992; Heywood, 1996) and enhances retention within the estuary by taking advantage of deep, landward advective currents at night that counteract seaward surface current movement during the day (Bosch & Taylor, 1973).

The zooplankton community in the York River was generally dominated year-round by *Acartia* copepods (*A. tonsa* and *A. hudsonica*), consistent with previous studies in the Chesapeake Bay and its tributaries (Kimmel et al., 2012; Cuker & Watson, 2002; Price, 1986). In addition to *Acartia* spp., the winter and spring zooplankton community

included high abundances of cladoceran *Podon polyphemoides* and barnacle nauplii. Though our data shows a peak in *P. polyphemoides* in the spring, long-term Chesapeake Bay zooplankton monitoring data suggests that *P. polyphemoides* typically peaks in July in the mouth of the York River (Steinberg & Condon, 2009). Annelids (mostly Spionid larvae) were abundant in the winter in the mesohaline site, and spring in the polyhaline site where they remained abundant through early fall. Non-*Acartia* calanoid copepod densities increased in February in the mesohaline site due to *Eurytemora affinis*, which has been observed to peak in abundance in the Chesapeake Bay in March/April (Kimmel & Roman, 2004; Steinberg & Condon, 2009). Mysids, isopods, larvaceans, and chaetognaths were abundant in the summer and fall in the polyhaline site; and larval meroplankton (decapods, phoronids, fishes, and mollusks) were also abundant in the summer, corresponding with the reported spawning season of many of these taxa from late spring through early fall (Marshall & Alden, 1985; Grant & Olney, 1983; Sandifer, 1973). Non-*Acartia* calanoid copepod (*Centropages* spp. and *Pseudodiaptomus* spp.) abundances increased in September, which is a typical seasonal pattern (Price, 1986). Gelatinous zooplankton peaked each summer, their typical "bloom" period in the York River (Condon & Steinberg, 2008) and Chesapeake Bay more broadly (Purcell et al., 1994; Stone et al., 2019). Ctenophores were most abundant in Nov. 2019 with a secondary peak in summer 2020, which is consistent with long-term observations of ctenophore abundance in the lower Bay that show a peak in June/July (Stone et al., 2019). Hydromedusae (especially *Nemopsis bachei*) were abundant throughout the sampling period and are key predators of *A. tonsa* copepodites and nauplii throughout the fall in the

southern Chesapeake Bay, thus competing for food with larval fishes and influencing fish recruitment (Purcell et al., 1999).

The importance of small size classes such as **Acartia** *spp. copepods to community fecal pellet carbon production*

Due to a lack of significant differences in weight-specific FPC production between size classes in community-level experiments, the relative contributions of each size class to total FPC production were directly correlated to the biomass of each size class. Thus, community FPC production was dominated by the smallest size class (0.2 – 0.5 mm) during daytime experiments with increasing relative contributions by larger size classes (particularly the 0.5 – 1 mm size class) at night due to diel vertical migration of larger animals into the surface. The 0.2 – 0.5 and 0.5 – 1 mm size classes were mainly comprised of *Acartia* spp. which dominated the zooplankton community, constituting up to 99% of total animal abundance, plus other smaller copepods.

Average carbon content of fecal pellets produced by *Acartia* spp. (0.29 µg C pellet^{-1}) in our individual species FPC production experiments was higher than in a previous study in the York River (0.02 µg C pellet^{-1}; Saba et al., 2011) but within the range of pellet carbon contents of *Acartia tonsa* feeding on large diatoms under simulated phytoplankton bloom conditions (0.03-0.38 µg C pellet^{-1}; Butler & Dam, 1994) and *Acartia hudsonica* feeding on coccolithophores (0.13-0.28 µg C pellet^{-1}; Honjo & Roman, 1978). The individual fecal pellet production rate of *Acartia* spp. in our study (0.25 pellets ind^{-1} hr^{-1}) is lower than previous studies of *Acartia tonsa* feeding on large

diatoms in the York River (2.8 pellets ind^{-1} hr^{-1}; Saba et al., 2011) and mixed calanoid copepod (including *Acartia* spp.) fecal pellet production rates in the Yangtze estuary in summer (0.62-1.34 pellets ind^{-1} hr^{-1}; Guo et al., 2018). Our mean per-individual pellet production rates may be comparatively lower due to differences in phytoplankton community structure compared to prior studies, or experimental artifacts such as settling of large diatoms causing food limitation in the jars or addition of small animals in ambient seawater that consumed phytoplankton or fecal pellets. Comparing studies on *Acartia* spp. FPC production rates is difficult due to the variety of units used in calculating production rates (most being calculated on an individual basis, µg C ind^{-1} hr^{-1}, or by carbon content of animals, µg C µg C^{-1} hr^{-1}). Our calculated mean individual FPC production rate for *Acartia* spp. (0.01-0.07 µg C ind^{-1} hr^{-1}) was similar to another coastal calanoid copepod, *Temora longicornis* (0.05-0.07 µg C ind^{-1} hr^{-1}; Ploug et al., 2008). However, weight-specific FPC production rates for *Acartia* spp. (mean = 3.9 µg C $mgDW^{-1}$ hr^{-1}) were nearly 4-fold higher than the small calanoid copepod *Clausocalanus lividus* (1.1 µg C $mgDW^{-1}$ hr^{-1}) in the Northeast Pacific Ocean (Stamieszkin et al., 2021).

The proportionately high contributions of < 1 mm size classes to overall community fecal pellet production are consistent with fecal pellet production studies in other estuaries and in the open ocean. Zooplankton in the 0.5 – 1 mm size class (dominated by calanoid copepods) produced over 50% of all fecal pellets in the highly productive Changjiang (Yangtze) estuary (Guo et al., 2018). In the subarctic Northeast Pacific Ocean, Stamieszkin et al. (2021) also show high contributions of small size classes to total community FPC production in the subarctic Northeast Pacific Ocean; there while the smallest size class (0.2 – 0.5 mm) contributed just 0.2-3% to total

biomass, it contributed the most (32%) to total community FPC production. This was partially due to high weight-specific FPC production rates, which generally decreased among taxa as organism size increased, but largely due to low FPC production rates by *Neocalanus* spp. copepods (which dominated the 2.0 – 5.0 mm size fraction) that were undergoing reduced feeding and gut shrinkage preceding their seasonal descent to diapause depths (Stamieszkin et al., 2021). In our study, although *Acartia* spp. had significantly lower individual FPC production rates than larger animals (mysids, isopods), high *Acartia* spp. density in the estuary leads to its dominance in community FPC production.

Large animals were likely underrepresented in community FPC production experiments due to their relative rareness, as well as evasion (due to faster swimming compared to smaller taxa) during subsampling for experiments that may have prevented them from being included in incubations. Taxon-specific FPC production experiments revealed that while larger animals (mysids and isopods) had lower weight-specific FPC production rates than *Acartia* spp., they had higher individual rates of FPC production (pellets ind^{-1} hr^{-1}) and created larger, more carbon-rich pellets. Contribution of these larger taxa to total community FPC production was thus likely underestimated, and care should be taken to target and include these animals in an appropriate concentration in future community-level FPC production experiments.

Diel differences in fecal pellet carbon production

Community FPC production rates were significantly higher (mean = 19-fold, range = 3- to 65-fold) in surface waters at night than during the day, driven by increases in biomass at night due to diel vertical migration of larger animals into the surface. This finding is consistent with the results of Stamieszkin et al. (2021) in the subarctic Northeast Pacific Ocean where FPC production at night was on average 3-fold that during the day. The biomass of the 0.5 – 1 mm and 1 – 2 mm size classes increased the most on average from day to night, due to migration of copepods, such as *Acartia* spp. and the larger *Centropages* spp. and *Pseudodiaptomus* spp., as well as chaetognaths, larval decapods, and fishes. *Acartia* spp. FPC production rate individual^{-1} was not significantly different between day and night, implying that feeding rates did not increase at night. Thus, increases in the abundance of *Acartia* spp. and other calanoid copepods in the surface at night likely drove the large increases in community FPC production from day to night. Biomass of the largest size class (> 5 mm) increased substantially between the day and night in the summer and fall due to the presence of mysids, which occurred in surface waters only at night. While mysids had relatively high FPC production rates, their abundance was relatively low compared to that of smaller animals such as copepods. The biomass of the > 5 mm size class also increased between day and night due to presence of large scyphozoans such as *Chrysaora chesapeakei* and *Aurelia aurita*. *Chrysaora* medusae show negative phototaxis (movement away from a directional light source) in both natural and manipulated light conditions in mesocosms (Schuyler & Sullivan, 1997), and *Aurelia aurita* vertically migrate into surface waters at dusk where they can produce swarms (Malej et al., 2007). Scyphomedusae were not included in fecal pellet production

experiments due to their size, but previous studies suggest they can play a significant role in top-down control of FPC flux in the Chesapeake Bay (Stone & Steinberg, 2018).

Diel differences in FPC production rates may have been affected by coprophagy (ingestion of fecal pellets) and coprorhexy (physical fragmentation of fecal pellets) by small (< 200 μm), seasonally abundant cladocerans and barnacle larvae, which were often found in the contents of the outer jars of fecal pellet production experiments along with filtered fecal pellets. Zooplankton in this size class play an important role in coprophagy and restricting vertical fecal pellet carbon flux (Poulsen & Kiørboe, 2006), thus their relatively higher abundance in the day potentially led to higher rates of coprophagy and coprorhexy in daytime fecal pellet production experiments, contributing to the observed relative increase in community FPC production rates from day to night.

Seasonal differences in fecal pellet carbon production

There was no significant difference between months in *Acartia* spp. FPC production rate individual^{-1} or in whole community FPC production. However, using FPC production rates from experiments in 2020 spanning several seasons along with monthly size-fractionated biomass measurements, we estimated seasonal differences in community FPC production in the polyhaline site. We split the sampling periods into three seasons: spring (Feb. – Apr.), summer (Jun. – Sept.), and fall (Oct. – Nov.), calculated the average daytime and nighttime biomass in each season, and applied weight-specific rates from community experiments to calculate daily rates of FPC production per size class for each season, which was integrated over the average depth of

the euphotic zone (3.1 m; Schultz, Jr., 1999) while considering changes in photoperiod (daylength). Daily community FPC production rates were highest in fall (866.2 mg C m^{-2} d^{-1}), intermediate in spring (444.1 mg C m^{-2} d^{-1}), and lowest in summer (301.3 mg C m^{-2} d^{-1}). Spring FPC production was dominated by the smallest, 0.2 – 0.5 mm size class (80% of total), while larger size classes contributed more to summer and fall FPC production. In the summer, the largest size class (> 5 mm) contributed 45% of daily FPC production due to high nighttime abundances of large animals (including mysids, chaetognaths, isopods, and hydrozoans). In the fall, the 1 – 2 mm size class contributed 50% of daily FPC production, driven by increases in the abundance of large non-*Acartia* calanoid copepods (*Pseudodiaptomus* spp. and *Centropages* spp.).

The comparatively lower summer community FPC production may be due to presence of gelatinous zooplankton, which can exert seasonal top-down control on FPC production through cascading trophic effects of the scyphozoan *Chrysaora chesapeakei* and ctenophore *Mnemiopsis leidyi* on copepods including *Acartia tonsa* (Stone & Steinberg, 2018). In mesocosm experiments in the York River, the presence of *M. leidyi* reduced their prey copepod densities, leading to a 50% decrease in copepod FPC flux (from 36 to 18 µg C m^{-3} d^{-1} without and with *M. leidyi*, respectively; Stone & Steinberg, 2018). However, *C. chesapeakei* preys on *M. leidyi*, thus when present in large numbers can reduce predation pressure on copepods and lead to increased copepod FPC production and flux. The relatively high abundance of ctenophores and hydrozoans, which are efficient predators of larval mesozooplankton including copepodites and barnacle nauplii (Purcell & Nemazie, 1992), in September 2020 may be partially responsible for lower rates of FPC production in the polyhaline site in the summer versus

fall and spring. In addition, while community FPC production experiments sometimes included ctenophores (*M. leidyi* and *Beroë ovata)*, it is difficult to identify the mucous masses egested after their feeding (versus 'proper' fecal pellets produced by other taxa), thus ctenophore fecal production is excluded in our experiments. Mesocosm experiments with ctenophores also show clearance rates increase with increasing mesocosm size (Purcell & Cowan Jr., 1995), thus the 4-liter incubation containers used in our experiments may not have been of sufficient volume for ctenophores to clear copepod prey, also leading to underestimation of the role of ctenophores in POC production in the summer and fall.

Implications for fecal pellet carbon vertical export in the York River

This study analyzed patterns of zooplankton FPC production, not the fate (vertical export) of this FPC, which must consider factors that affect attenuation of sinking particles. FPC production is thus the maximum possible POC available for export to depth from surface waters. Applying average photoperiod (day/night lengths) to our data and integrating over the average depth of the euphotic zone (3.1 m; Schultz, Jr., 1999), our estimate of FPC production in polyhaline York River surface waters (mean: 928 mg C m^{-2} d^{-1}, range: 699-1158 mg C m^{-2} d^{-1}) is a maximum estimate of potential flux if no pellets are attenuated within the water column. For comparison, in the Yangtze estuary mean potential FPC flux from mixed copepods ranged from 34.6-64.4 mg C m^{-2} d^{-1} in the spring and 51.8-89.0 mg C m^{-2} d^{-1} in the summer (Guo et al., 2018). Their study was based on vertical net tows performed from 5 m above the sediment floor to the surface, and the FPC values are substantially lower than in our study likely due to exclusion of

non-copepod taxa and migrators, including copepods, that spend daylight hours within or near the sediment floor. Further, our estimate of community FPC production is two orders of magnitude higher than in a study using the same methods in the subarctic Northeast Pacific Ocean (mean: 3.1 mg C m^{-2} d^{-1}), which represents a low flux end-member of the biological pump as an open ocean, high nutrient-low chlorophyll (HNLC) region (Stamieszkin et al., 2021). In the Northeast Pacific Ocean, average biomass of zooplankton in the euphotic zone was roughly half of the biomass in the euphotic zone in our study. Thus, the higher rates of community FPC production in our study can be attributed to higher zooplankton biomass as well as low fecal pellet production rates by the dominant copepod, *Neocalanus* spp., in the Northeast Pacific (Stamieszkin et al. 2021).

Factors that control the attenuation or fate of these zooplankton fecal pellets produced in surface waters include pellet sinking rate variability, coprophagy (consumption of pellets) and coprophexy (fragmentation of pellets), and bacterial remineralization (Lampitt et al., 1990; Poulsen & Kiørboe, 2006; Stukel et al., 2011). In estuaries, physical processes such as resuspension and flushing due to river flow and the tidal cycle are also important. Coprophagy of fecal pellets by zooplankton plays a particularly important role in attenuation of fecal pellets in regions dominated by small copepods, such as the strait of Øresund between Denmark and Sweden, where most pellets produced in the surface were attenuated within the upper 50 m of the water column (Poulsen & Kiørboe, 2006). In the subarctic Northeast Pacific, sediment trap analysis revealed that fecal pellets egested from small mesozooplankton are highly abundant within the upper epipelagic zone but are attenuated rapidly with depth (on

average 86% were attenuated by 100 m), therefore contributing little to total POC flux to the mesopelagic zone (Stamieszkin et al., 2021; Durkin et al., 2021). Sediment trap studies in estuaries that quantify vertical FPC export reveal up to 1.3% of total POC in traps at depths of 10-50 m can be attributed to FPC, with the majority of POC being detritus (Svensen et al., 2007; Waite et al., 2005). The sediment trap depths in these estuarine studies are deeper than the York River – which has main channel depths ranging from 6 m to 24 m (Friedrichs, 2009), thus the relative magnitude of FPC export in the York River is likely more tightly coupled to surface FPC production due to less area for attenuation within the water column.

Comparison to net primary production (NPP) in the York River provides further context for our results. Our mean estimate for FPC production (0.93 g C m^{-2} d^{-1}), and thus potential FPC export, falls mid-range of direct measurements of summer water column NPP (0.43 – 1.66 g C m^{-2} d^{-1}; Lake et al., 2013), exceeds modeled mean seasonal estimates of NPP (0.37 g C m^{-2} d^{-1} in fall and 0.88 g C m^{-2} d^{-1} in spring and summer; Lake & Brush, 2015), and is one-quarter of maximum spring NPP (model estimate: 3.64 g C m^{-2} d^{-1}; Lake & Brush, 2015). While ultimately maximum FPC production (and export) cannot exceed NPP (particle production), the time scales of these measurements are different, and this comparison shows potential for significant vertical export of NPP as FPC.

5. CONCLUSIONS AND FUTURE CONSIDERATIONS

Estuaries such as the Chesapeake Bay and its tributaries can surpass oceanic systems in terms of their contribution to FPC production due to relatively high densities

of small zooplankton. While measurements from the Northeast Pacific (with consistent methods) represent a low-flux end member, comparisons between the results of this study and that of the Northeast Pacific show that estuaries can display a higher rate of POC production and potential vertical export of carbon than open ocean systems, which are more frequently studied regarding their role in the biological carbon pump.

This study focused on production of zooplankton fecal pellets, not their sinking rates or fate. Understanding the processes that contribute to fecal pellet attenuation in estuaries is critical in determining the role of fecal pellet production in vertical carbon export. Further, this study did not account for active transport of FPC to depth by diel migrating species (e.g., Schnetzer & Steinberg, 2002). Our study suggests that consideration of the diel cycle is critical for understanding diel and seasonal changes in potential FPC flux in estuaries, particularly because some of the most abundant taxa are diel vertical migrators. Sediment trap studies in estuaries that include techniques such as polyacrylamide gel traps for gentle collection of intact particles enabling classification of particle types (e.g., Durkin et al., 2021), as well as discrete multiple-depth, diel sampling of zooplankton, would help to determine the fate of fecal pellets produced in the surface waters and their contribution to estuarine benthic-pelagic coupling.

This study provides a baseline for future analysis of long-term changes in zooplankton community structure and carbon cycling in the Chesapeake Bay region. Beaugrand et al. (2010) showed long-term latitudinal changes in copepod biodiversity and their fecal pellet surface residence time in the North Atlantic, with copepod diversity increasing over time in the northern latitudes due to increasing water temperatures and species range extensions. A linear multiregression model indicated copepod body size

was negatively correlated with diversity, suggesting an overall decrease in copepod body size leading to smaller, more slowly sinking fecal pellets, which remain in surface waters longer (Beaugrand et al., 2010). Increased residence time of pellets in the epipelagic zone increases the likelihood of remineralization and decreases the likelihood of carbon burial and sequestration, which can have a profound impact on the ocean carbon cycle and our climate system. Estuaries are expected to be similarly impacted by climate change (Irby et al., 2018), with projected increases in water temperature over time, but also sea level rise causing shifts in the salinity regime and a variety of factors influencing dissolved oxygen concentration throughout the water column. These changes would collectively affect zooplankton horizontal and vertical distribution, as well as survival, and thus zooplankton-mediated carbon cycling. The role of the biological pump in estuaries has rarely been examined, but is needed to improve carbon cycling models, and to understand the effects of climate change on estuarine ecosystems.

LITERATURE CITED

Anderson, T.R. & Tang, K.W. (2010). Carbon cycling and POC turnover in the mesopelagic zone of the ocean: insights from a simple model. *Deep Sea Research II, 57*, 1581-1592.

Atkinson, D. (1994). Temperature and organism size: a biological law for ectotherms? *Advances in Ecology Research, 25*, 1-58.

Beaugrand, G., Edwards, M., & Legendre, L. (2010). Marine biodiversity, ecosystem functioning, and carbon cycles. *Proceedings of the National Academy of Sciences of the United States of America, 107*(22), 10120-10124. doi: 10.1073/pnas.0913855107

Berelson, W.M. (2001). The flux of particulate organic carbon into the ocean interior: a comparison of four U.S. JGOFS regional studies. *Oceanography, 14*(4), 59-67.

Bollens, S.M., Frost, B.W., Thoreson, D.S., & Watts, S.J. (1992). Diel vertical migration in zooplankton: field evidence in support of the predator avoidance hypothesis. *Hydrobiologia, 234*, 33-39.

Bosch, H.F. and Taylor, W.R. (1973). Diurnal vertical migration of an estuarine cladoceran, *Podon polyphemoides*, in the Chesapeake Bay. *Marine Biology, 19*(2), 172-181. doi: 10.1007/BF00353589

Bucklin, A., Ortman, B.D., Jennings, R.M., Nigro, L.M., Sweetman, C.J., Copley, N.J., Sutton, T., & Wiebe, P.H. (2010). A "Rosetta Stone" for metazoan zooplankton: DNA barcode analysis of species diversity of the Sargasso Sea (Northwest Atlantic Ocean). *Deep Sea Research II, 57*(24-26), 2234-2247. doi: 10.1016/j.dsr2.2010.09.025

Burd, A.B., Hansell, D.A, Steinberg, D.K., Anderson, T.R., Arístegui, J., Baltar, F., Beaupré, S.R., Buesseler, K.O., DeHairs, F., Jackson, G.A., Kadko, D.C., Koppelmann, R., Lampitt, R.S., Nagata, T., Reinthaler, T., Bobinson, C.,

Robison, B.H., Tamburini, C., & Tanaka, T. (2010). Assessing the apparent imbalance between geochemical activity and biochemical indicators of meso- and bathypelagic biological activity: what the @$#! is wrong with present calculations of carbon budgets? *Deep-Sea Research II, 57*, 1557- 1571.

Butler, M., & Dam, H.G. (1994). Production rates and characteristics of fecal pellets of the copepod *Acartia tonsa* under simulated phytoplankton bloom conditions: implications for vertical fluxes. *Marine Ecology Progress Series, 114*, 81-91.

Calliari, D., Cervetto, G., & Gomez, M. (2001). Short-term variability in abundance and vertical distribution of the opossum shrimp *Neomysis americana* in the Solís Grande River Estuary, Uruguay. *Atlanticâ, 23*, 117-125.

Chazarreta, J., Hoffmeyer, M. S., Cuadrado, D. G., & Berasategui, A. A. (2015). Tidal effects on short-term mesozooplankton distribution in small channels of a temperate-turbid estuary, Southwestern Atlantic. *Brazilian Journal of Oceanography, 63*(2), 83–92. doi: 10.1590/s1679-87592015076806302

Chew, L., Chong, V.C., Ooi, A.L., & Sasekumar, A. (2015). Vertical migration and positioning behavior of copepods in a mangrove estuary: Interactions between tidal, diel light and lunar cycles. *Estuarine, Coastal, and Shelf Science, 152*, 142-152. doi: 10.1016/j.ecss.2014.11.011

Cohen, J.H. & Forward Jr., R.B. (2009). Zooplankton Diel Vertical Migration – A Review of Proximate Control. *Oceanogr. Mar. Biol. Annu. Rev., 47*, 77–109. doi: 10.1201/9781420094220.ch2

Condon, R.H. & Steinberg, D.K. (2008). Development, biological regulation, and fate of ctenophore blooms in the York River estuary, Chesapeake Bay. *Marine Ecology Progress Series, 369*, 153-168. doi: 10.3354/meps07595

Cuker, B. E., & Watson, M. A. (2002). Diel vertical migration of zooplankton in contrasting habitats of the Chesapeake Bay. *Estuaries, 25*(2), 296-307. doi: 10.1007/bf02691317

Cyr, H. & Pace, M.L. (1993). Allometric theory: Extrapolations from individuals to communities. *Ecology*, *74*(4). doi: 10.2307/1940493

Dagg, M. J., Jackson, G.A., & Checkley, D.M. (2014). The distribution and vertical flux of fecal pellets from large zooplankton in Monterey Bay and coastal California. *Deep-Sea Research I, 94*, 72-86. doi: 10.1016/j.dsr.2014.09.001

Dawidowicz, P., & Pijanowska, J. (2018). Diel vertical migration of aquatic crustaceans—adaptive role, underlying mechanisms, and ecosystem consequences. In: *The Natural History of the Crustacea: Life Histories*, pp. 231-256.

Deevey, G.B. (1971). The annual cycle in quantity and composition of the zooplankton of the Sargasso Sea off Bermuda. *ASLO Limnology and Oceanography, 16*(2), 219-240. Doi: 10.4319/lo.1971.16.2.0219

Derisio, C., Braverman, M., Gaitán, E., Hozbor, C., Ramírez, F., Carreto, J., Botto, F., Gagliardini, D.A., Acha, E.M., & Mianzan, H. (2014). The turbidity front as a habitat for *Acartia tonsa* (Copepoda) in the Río de la Plata, Argentina-Uruguay. *Journal of Sea Research, 85*, 197-204.

Durkin, C.A., Buesseler, K.O., Cetinić, I., Estapa, M.L., Kelly, R.P., & Omand, M. (2021). A visual tour of carbon export by sinking particles. *AGU Global Biogeochemical Cycles*. doi: 10.1029/2021GB006985

Friedrichs, C.T. (2009) York River physical oceanography and sediment transport. *Journal of Coastal Research, 10057*, 17-22. doi: 10.2112/1551-5036-57.sp1.17

Gleiber, M.R., Steinberg, D.K., & Ducklow, H. (2012). Time series of vertical flux of zooplankton fecal pellets on the continental shelf of the Western Antarctic Peninsula. *Marine Ecology Progress Series, 471*, 23-36. doi: 10.3354/meps10021

Grant, G. C. & Olney, J. E. (1983). Lower Bay zooplankton monitoring program: the August 1978 survey. Special scientific report No. 115. Virginia Institute of

Marine Science, College of William and Mary. Retrieved from: http://dx.doi.org/doi:10.21220/m2-9b0m-k225

Guo, S., & Sun, X. (2018). Carbon biomass, production rates and export flux of copepods fecal pellets in the Changjiang (Yangtze) River estuary. *Journal of Oceanology and Limnology, 36*(4), 1244–1254. doi: 10.1007/s00343-018-7057-1

Haraldsson, M., Båmstedt, U., Tiselius, P., Titelman, J., & Aksnes, D. L. (2014). Evidence of diel vertical migration in Mnemiopsis leidyi. *PloS one, 9*(1), e86595. doi: 10.1371/journal.pone.0086595

Harding, L. W., Mallonee, M.E, & Perry, E.S. (2002). Toward a Predictive Understanding of Primary Productivity in a Temperate, Partially Stratified Estuary. *Estuarine, Coastal and Shelf Science, 55*(3), 437-463.

Hays, G.C. (2003). A review of the adaptive significance and ecosystem consequences of zooplankton diel vertical migrations. In: *Migrations and Dispersal of Marine Organisms*, Springer, (pp. 163-170). doi: 10.1007/978-94-017-2276-6_18

Henson, S., Le Moigne, F., & Giering, S. (2019). Drivers of Carbon Export Efficiency in the Global Ocean. *Global Biogeochemical Cycles, 33*(7), 891-903. doi: 10.1029/2018GB006158

Hessen, D.O., Bakkestuen, V., & Walseng, B. (2007). Energy input and zooplankton species richness. *Ecography, 30,* 749-758. doi: 10.1111/j.2007.0906-7590.05259.x4

Holliland, P.B., Ahlbeck, I., Westlund, E., & Hansson, S. (2012). Ontogenetic and seasonal changes in diel vertical migration amplitude of the calanoid copepods *Eurytemora affinis* and *Acartia* spp. in a coastal area of the northern Baltic proper. *Journal of Plankton Research, 34*(4), 298-307. doi: 10.1093/plankt/fbs001

Honjo, S. & Roman, M.R. (1978). Marine copepod fecal pellets: production, preservation and sedimentation. *Journal of Marine Research, 36,* 45-57.

Irby, I.D., Friedrichs, M. A.M., Da, F., & Hinson, K.E. (2018). The competing impacts of climate change and nutrient reductions on dissolved oxygen in Chesapeake Bay. *Biogeosciences, 15*, 2649-2668. doi: 10.5194/bg-15-2649-2018

Kehayias, G. & Ntakou, E. (2008). Abundance, vertical distribution and feeding of chaetognaths in the upper 50 m layer of the Aegean Sea. *Journal of Natural History, 42*, 633-648. doi: 10.1080/00222930701835597

Kehayias, G. & Kourouvakalis, D. (2010). Diel vertical migration and feeding of chaetognaths in coastal waters of the eastern Mediterranean. *Biologia, 65*(2), 301-308. doi: 10.2478/s11756-010-0024-8

Kelly, T.B., Davison, P.C., Goericke, R., Landry, M.R., Ohman, M.D., & Stukel, M.R. (2019). The importance of mesozooplankton diel vertical migration for sustaining a mesopelagic food web. *Frontiers in Marine Science, 6*. doi: 10.3389/fmars.2019.00508

Kimmel, D.G., Boynton,W.R., & Roman, M.R. (2012). Long-term decline in the calanoid copepod *Acartia tonsa* in Central Chesapeake Bay, USA: An indirect effect of eutrophication? *Estuarine, Coastal and Shelf Science, 101*, 76–85. doi: 10.1016/j.ecss.2012.02.019

Kimmerer, W.J., Burau, J.R., & Bennett, W.A. (2002). Persistence of tidally-oriented vertical migration by zooplankton in a temperate estuary. *Estuaries, 25,* 359-371.

Lake, S.J., Brush, M.J., Anderson, I.C., & Kator, H.I. (2013). Internal versus external drivers of periodic hypoxia in a coastal plain tributary estuary: the York River, Virginia. *Marine Ecology Progress Series, 492*, 21-39. doi: 10.3354/meps10468

Lake, S.J. & Brush, M.J. (2015). Modeling estuarine response to load reductions in a warmer climate: York River Estuary, Virginia, USA. *Marine Ecology Progress Series, 538*, 81-98. doi: 10.3354/meps11448

Lampitt, R.S., Noji, T. & von Bodungen, B. (1990). What happens to zooplankton faecal

pellets? Implications for material flux. *Marine Biology, 104,* 15-23.

Lomas, M.W., Bates, N.R., Johnson, R.J., Knap, A.H., Steinberg, D.K., & Carlson, C.A. (2013). Two decades and counting: 24-years of sustained open ocean biogeochemical measurements in the Sargasso Sea. *Deep Sea Research II, 93,* 16-32. doi: 10.1016/j.dsr2.2013.01.008

Ludsin, S.A., Zhang, X., Brandt, S.B., Roman, M.R., Boicourt, W.C., Mason, D.M., & Costantini, M. (2009). Hypoxia-avoidance by planktivorous fish in Chesapeake Bay: Implications for food web interactions and fish recruitment. *Journal of Experimental Marine Biology and Ecology, 381*(supplement): S121-S131. doi: 10.1016/j.jembe.2009.07.016

Madin, L.P., Horgan, E.F., & Steinberg, D.K. (2001*).* Zooplankton at the Bermuda Atlantic Time-series Study (BATS) station: diel, seasonal and interannual variation in biomass, 1994-1998. *Deep-Sea Research II, 48*(8-9): 2063-2082.

Makarieva, A.M., Gorshkov, V.G., Li, B., Chown, S.L., Reich, P.B., & Gavrilov, V.M. (2008). Mean mass-specific metabolic rates are strikingly similar across life's major domains: Evidence for life's metabolic optimum. *Proceedings of the National Academy of Sciences of the United States of America, 105*(44), 16994-16999. doi: 10.1073/pnas.0802148105

Malej, A., Turk, V., Lučić, D., & Benović, A. (2007). Direct and indirect trophic interactions of *Aurelia* sp. (Scyphozoa) in a stratified marine environment (Mijet Lakes, Adriatic Sea). *Marine Biology, 151*(3), 827-841. doi: 10.1007/s00227-006-0503-1

Marshall, H.G. & Alden III, R.W. (1985). Seasonal relationships between phytoplankton and mero-zooplankton populations in the Lower Chesapeake Bay, Virginia. Final report No. ADA165037. US Army Corps of Engineers, Norfolk Division.

Naylor, E. (2006). Orientation and navigation in coastal and estuarine zooplankton. *Marine and Freshwater Behaviour and Physiology, 39,* 13-24. doi:

10.1080/10236240600593344

Nixon S.W. (1981). Remineralization and nutrient cycling in coastal marine ecosystems. In *Estuaries and Nutrients* (pp. 111–138).

Nogueira Júnior, M., Brandini, F. P., & Codina, J. C. (2015). Diel Vertical Dynamics of Gelatinous Zooplankton (Cnidaria, Ctenophora and Thaliacea) in a Subtropical Stratified Ecosystem (South Brazilian Bight). *PloS one*, *10*(12), e0144161. doi: 10.1371/journal.pone.0144161

North, E.W. & Houde, E.D. (2004). Distribution and transport of bay anchovy (*Anchoa mitchilli*) eggs and larvae in Chesapeake Bay. *Estuarine, Coastal and Shelf Science, 60*(3), 409-429. doi: 10.1016/j.ecss.2004.01.011

Park, G.S. & Marshall, H.G. (2000). Estuarine relationships between zooplankton community structure and trophic gradients. *Journal of Plankton Research, 22*(1), 121-136. doi: 10.1093/plankt/22.1.121

Parra, S.M., Greer, A.T., Book, J.W., Deary, A.L., Soto, I.M., Culpepper, C., Hernandex, F.J., & Miles, T.N. (2019). Acoustic detection of zooplankton diel vertical migration behaviors on the northern Gulf of Mexico shelf. *Limnology and Oceanography, 64*(5), 2092-2113. doi: 10.1002/lno.11171

Pinckney, J.L., Paerl, H.W., Tester, P., & Richardson, T.L. (2001). The role of nutrient loading and eutrophication in estuarine ecology. *Environmental Health Perspectives, 109*(5), 699-706. doi: 10.2307/3454916

Ploug, H., Iversen, M.H., Koski, M., & Buitenhuis, E.T. (2008). Production, oxygen respiration rates, and sinking velocity of copepod fecal pellets: Direct measurements of ballasting by opal and calcite. *Limnology and Oceanography, 53*(2), 469-476. doi: 10.4319/lo.2008.53.2.0469

Postel, L., Fock, H., & Hagen, W. (2000). 4 - Biomass and abundance. In *ICES Zooplankton Methodology Manual* (pp. 83–192). doi: 10.1016/B978-012327645-

2/50005-0

Poulsen, L.K. & Kiørbe, T. (2006). Vertical flux and degradation rates of copepod fecal pellets in a zooplankton community dominated by small copepods. *Marine Ecology Progress Series, 323,* 195-204.

Price, J.E. (1986). Estuarine zooplankton community structure in stratified and well-mixed environments. *PhD Dissertation, William & Mary School of Marine Science*. Available from ProQuest Dissertations & Theses Global. (303553931).

Purcell, J.E. & Nemazie, D.A. (1992). Quantitative feeding ecology of the hydromedusan *Nemopsis bachei* in Chesapeake Bay. *Marine Biology, 113,* 305-311.

Purcell, J.E., White, J.R., & Roman, M.R. (1994). Predation by gelatinous zooplankton and resource limitation as potential controls of *Acartia tonsa* copepod populations in Chesapeake Bay. *Limnology and Oceanography, 39*(2), 263-278.

Purcell, J.E. & Cowan Jr., J.H. (1995). Predation by the scyphomedusan *Chrysaora quinquecirrha* on *Mnemiopsis leidyi* ctenophores. *Marine Ecology Progress Series, 129,* 63-70. doi: 10.3354/meps129063

Purcell, J.E., Malej, A., & Benović, A. (1999). Potential links of jellyfish to eutrophication and fisheries. *Ecosystems at the Land-Sea Margin: Drainage Basin to Coastal Sea, 55,* 241-263. In *Coastal and Estuarine Studies*.

Reay, W. G. (2009). Water Quality within the York River Estuary. *Journal of Coastal Research, 10057,* 23-39. doi: 10.2112/1551-5036-57.sp1.23

Riser, C.W., Reigstad, M. & Wassmann, P. (2010). Zooplankton-mediated carbon export: A seasonal study in a northern Norwegian fjord. *Marine Biology Research, 6*:5, 461-471. doi: 10.1080/17451000903437067

Roman, M.R., Holliday, D.V., & Sanford, L.P. (2001). Temporal and spatial patterns of zooplankton in the Chesapeake Bay turbidity maximum. *Marine Ecology Progress Series, 213,* 215-227. doi: 10.3354/meps213215

Saba, G.K., Steinberg, D.K., & Bronk, D.A. (2011). The relative importance of sloppy feeding, excretion, and fecal pellet leaching in release of dissolved carbon and nitrogen by *Acartia tonsa* copepods. *Journal of Experimental Marine Biology and Ecology, 404*, 47-56. doi: 10.1016/j.jembe.2011.04.013

Sanders, R., Henson, S. A, Koski, M., De La Rocha, C. L., Painter, S.C., Poulton, A.J., Riley, J., Salihoglu, B., Visser, A., Yool, A., Bellerby, R., & Martin, A.P. (2014). The Biological Carbon Pump in the North Atlantic. *Progress in Oceanography, 129*(B), 200-218. doi: 10.1016/j.pocean.2014.05.005

Sandifer, P.A. (1973). Distribution and abundance of decapod crustacean larvae in the York River Estuary and adjacent Lower Chesapeake Bay, Virginia, 1968-1969. *Chesapeake Science, 14*(4), 235-257. doi: 10.2307/1350753

Schnetzer, A. & Steinberg, D.K. (2002). Active transport of particulate organic carbon and nitrogen by vertically migrating zooplankton in the Sargasso Sea. *Marine Ecology Progress Series, 234*, 71-84. doi: 10.3354/meps234071

Schuyler, Q. & Sullivan, B.K. (1997). Light responses and diel migration of the scyphomedusa *Chrysaora quinquecirrha* in mesocosms. *Journal of Plankton Research, 19*(10), 1417-1428. doi: 10.1093/plankt/19.10.1417

Schultz, G. E., Jr. (1999). Bacterial dynamics and community structure in the York River estuary. *PhD Dissertation, College of William & Mary School of Marine Science*. Available from ProQuest Dissertations & Theses Global. (304535494).

Shoaf, W.M. & Lium, B.W. (1976). Improved extraction of chlorophyll a and b from algae using dimethyl sulfoxide. *Limnology and Oceanography, 21*(6), 926-928. doi: 10.4319/lo.1976.21.6.0926

Stamieszkin, K., Steinberg, D.K., & Maas, A. (2021). Fecal pellet production by mesozooplankton in the subarctic Northeast Pacific Ocean. *Limnology and Oceanography, 66*(7), 2585-2597. doi: 10.1002/lno.11774

Steinberg, D.K., and Condon, R.H. (2009). Zooplankton of the York River. *Journal of Coastal Research, Special issue No. 57*: 66-79.

Steinberg, D. K., & Landry, M. R. (2017). Zooplankton and the Ocean Carbon Cycle. *Annual Review of Marine Science, 9*(1), 413-444. doi: 10.1146/annurev-marine-010814-015924

Steinberg, D. K., Lomas, M. W., & Cope, J. S. (2012). Long-term increase in mesozooplankton biomass in the Sargasso Sea: Linkage to climate and implications for food web dynamics and biogeochemical cycling. *Global Biogeochemical Cycles, 26*(1). doi: 10.1029/2010gb004026

Stone, J. & Steinberg, D.K. (2014). Long-term time-series study of salp population dynamics in the Sargasso Sea. *Marine Ecology Progress Series, 510*, 111-127. doi: 10.3354/meps10985

Stone, J. & Steinberg, D.K. (2018). Influence of top-down control in the plankton food web on vertical carbon flux: A case study in the Chesapeake Bay. *Journal of Experimental Marine Biology and Ecology, 498*, 16-24. doi: 10.1016/j.jembe.2017.10.008

Stone J. P., Steinberg, D.K. & Fabrizio, M.C. (2019). Long-term changes in gelatinous zooplankton in Chesapeake Bay, USA: Environmental controls and interspecific interactions. *Estuaries and Coasts, 42*, 513-527. doi: 10.1007/s12237-018-0459-7

Stukel, M.R., Landry, M.R., Benitez-Nelson, C.R., & Goericke, R. (2011). Trophic cycling and carbon export relationships in the California Current Ecosystem. *Limnology and Oceanography, 56*(5), 1866-1878. doi: 10.4319/lo.2911.56.5.1866

Stukel, M.R., Ohman, M.D., Benitez-Nelson, C.R., & Landry, M.R. (2013). Contributions of mesozooplankton to vertical carbon export in a coastal upwelling system. *Marine Ecology Progress Series, 491*, 47–65.

Svensen, C., Viličić, D., Wassmann, P., Arashkevich, E., & Ratkova, T. (2007). Plankton

distribution and vertical flux of biogenic matter during high summer stratification in the Krka estuary (Eastern Adriatic). *Estuarine, Coastal and Shelf Science, 71*(3-4), 381–390. doi: 10.1016/j.ecss.2006.07.022

Sweetman, C.J. (2018). Consumption patterns of Chesapeake Bay fishes. *PhD Dissertation, College of William & Mary School of Marine Science*.

Turner, J. T. (2015). Zooplankton fecal pellets, marine snow, phytodetritus and the ocean's biological pump. *Progress in Oceanography,130*, 205-248. doi: 10.1016/j.pocean.2014.08.005

Urban-Rich, J. (2001). Seston effects on faecal pellet carbon concentrations from a mixed community of copepods in Balsfjord, Norway, and the Antarctic Polar Front. *ICES Journal of Marine Science, 58*(3), 700-710. doi:10.1006/jmsc.2000.1055

Valentin, J.L., Marazzo, A., & Gomes, C.L. (2003). The diel vertical migration pattern of the cladoceran *Pleopis polyphemoides* (Leuckart, 1859) in a stratified tropical bay. *Crustaceana, 76*(5), 513-521.

Vineetha, G., Jyothibabu, R., Madhu, N.V., Kusum, K.K., Sooria, P.M., Shivaprasad, A., Reny, P.D., & Deepak, M.P. (2015). Tidal influence on the diel vertical migration pattern of zooplankton in a tropical monsoonal estuary. *Wetlands, 35*, 597-610.

Waite, A. M., Gustafsson, Ö., Lindahl, O., & Tiselius, P. (2005). Linking ecosystem dynamics and biogeochemistry: Sinking fractionation of organic carbon in a Swedish fjord. *Limnology and Oceanography*, 50(2), 658–671. doi: 10.4319/lo.2005.50.2.0658

Wilson, S.E., Steinberg, D.K., & Buesseler, K.O. (2008). Changes in fecal pellet characteristics with depth as indicators of zooplankton repackaging of particles in the mesopelagic zone of the subtropical and subarctic North Pacific Ocean. *Deep Sea Research II, 55*, 1636–47.

Table 1. List of major taxa identified from York River zooplankton samples. Copepoda includes the most abundant calanoid copepod genus, *Acartia* (*A. tonsa* and *A. hudsonica*), all other calanoid copepods combined, and three other orders of copepods. Balanidae includes barnacle larvae (both nauplius and cyprid stages). Cnidaria includes two classes: "true jellyfish" scyphozoans with large free-living medusae such as bay nettles, and relatively smaller (< 10 mm) predatory hydrozoans (nearly exclusively *Nemopsis bachei*). Teleostei includes larval fishes.

Taxonomic Categories	**Sub-Categories**
Copepoda	*Acartia* spp.
	Other Calanoida
	Cyclopoida
	Harpacticoida
	Siphonostomatoida
Cladocera	
Balanidae	
Decapoda	
Mysidacea	
Isopoda	
Ctenophora	
Cnidaria	Scyphozoa
	Hydrozoa
Mollusca	
Chaetognatha	
Annelida	
Phoronida	
Larvacea	
Teleostei	

Table 2. Summary table of results of individual taxon-specific fecal pellet production experiments. Values are mean ± standard error (SE).

Taxa	No. of experiments	Day / Night	Mean FP volume ± SE (mm^3)	Mean FPC vol^{-1} ± SE ($mg\ mm^{-3}$)	Mean C FP^{-1} ± SE ($\mu g\ pellet^{-1}$)	Mean FPC production rate ± SE ($\mu g\ C\ ind^{-1}\ hr^{-1}$)	Mean weight-specific FPC production rate ± SE ($\mu g\ C\ mgDW^{-1}\ hr^{-1}$)
Acartia spp.	-	-	$1.25 \times 10^{-3} \pm 2.07 \times 10^{-4}$	0.55 ± 0.13	0.29 ± 0.04	0.04 ± 0.01	3.85 ± 0.37
-	6	Day	$1.40 \times 10^{-3} \pm 2.68 \times 10^{-4}$	0.32 ± 0.08	0.24 ± 0.07	0.03 ± 0.01	4.05 ± 1.22
-	4	Night	$1.00 \times 10^{-3} \pm 3.31 \times 10^{-4}$	0.92 ± 0.29	0.36 ± 0.06	0.03 ± 0.01	3.10 ± 0.86
Mysidacea (*Neomysis americana*)	2	Night	$2.98 \times 10^{-3} \pm 1.62 \times 10^{-3}$	0.42 ± 0.21	0.52 ± 0.10	0.43 ± 0.09	0.44 ± 0.25
Isopod (*Livoneca redmanii*)	2	Night	$4.79 \times 10^{-4} \pm 8.38 \times 10^{-5}$	1.21 ± 0.56	0.67 ± 0.42	0.24 ± 0.10	0.01 ± 0.003

Table 3. Summary table of results of community-level fecal pellet production experiments. Values are mean ± standard error (SE). Mean C FP^{-1} was calculated from mean FP volume and mean FPC vol^{-1} when a direct measurement was not possible.

Size Fraction	Mean FP volume ± SE (mm^3)	Mean FPC vol^{-1} ± SE (mg mm^{-3})	Mean C FP^{-1} ± SE (µg $pellet^{-1}$)	Mean FPC production rate ± SE (mg C $mgDW^{-1}$ hr^{-1})
0.2 – 0.5 mm	$4.44 \times 10^{-4} \pm 7.42 \times 10^{-5}$ *(n=22)*	0.29 ± 0.11 *(n=17)*	$8.33 \times 10^{-5} \pm 2.92 \times 10^{-5}$ *(n=22)*	0.35 ± 0.11 *(n=11)*
0.5 – 1 mm	$5.90 \times 10^{-4} \pm 8.08 \times 10^{-5}$ *(n=22)*	0.14 ± 0.02 *(n=9)*	$7.41 \times 10^{-5} \pm 1.01 \times 10^{-5}$ *(n=18)*	0.35 ± 0.07 *(n=11)*
1 – 2 mm	$8.32 \times 10^{-4} \pm 1.58 \times 10^{-4}$ *(n=22)*	0.17 ± 0.08 *(n=13)*	$1.59 \times 10^{-4} \pm 5.49 \times 10^{-5}$ *(n=21)*	0.36 ± 0.10 *(n=11)*
2 – 5 mm	$8.89 \times 10^{-4} \pm 1.59 \times 10^{-4}$ *(n=22)*	0.14 ± 0.07 *(n=9)*	$1.02 \times 10^{-4} \pm 1.95 \times 10^{-5}$ *(n=19)*	0.19 ± 0.04 *(n=11)*
> 5 mm	$8.74 \times 10^{-4} \pm 1.16 \times 10^{-4}$ *(n=22)*	0.29 ± 0.10 *(n=8)*	$4.52 \times 10^{-4} \pm 1.01 \times 10^{-4}$ *(n=17)*	0.33 ± 0.05 *(n=11)*

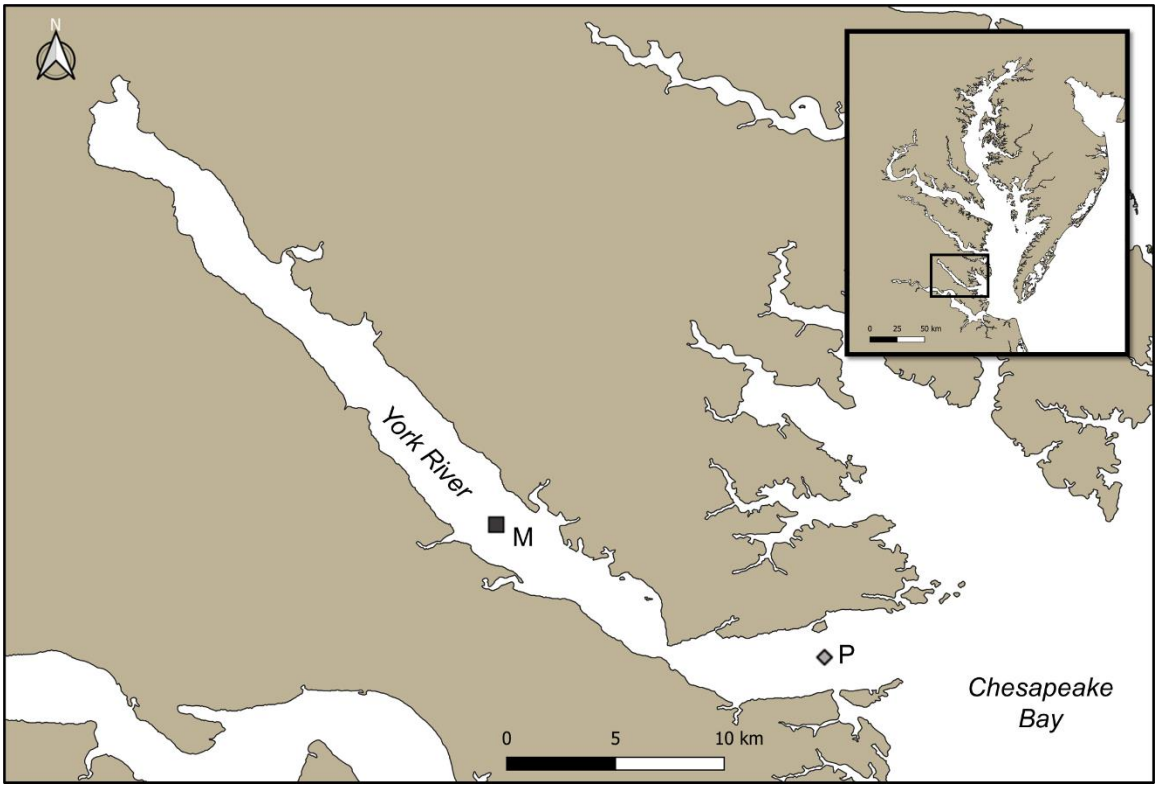

Figure 1. Sampling sites in York River, Chesapeake Bay. Upriver mesohaline site (M; depth = 10.4 m) and downriver polyhaline site (P; depth = 16.8 m) are denoted by dark grey square and light grey diamond, respectively. Location of York River within Chesapeake Bay region shown in inset map.

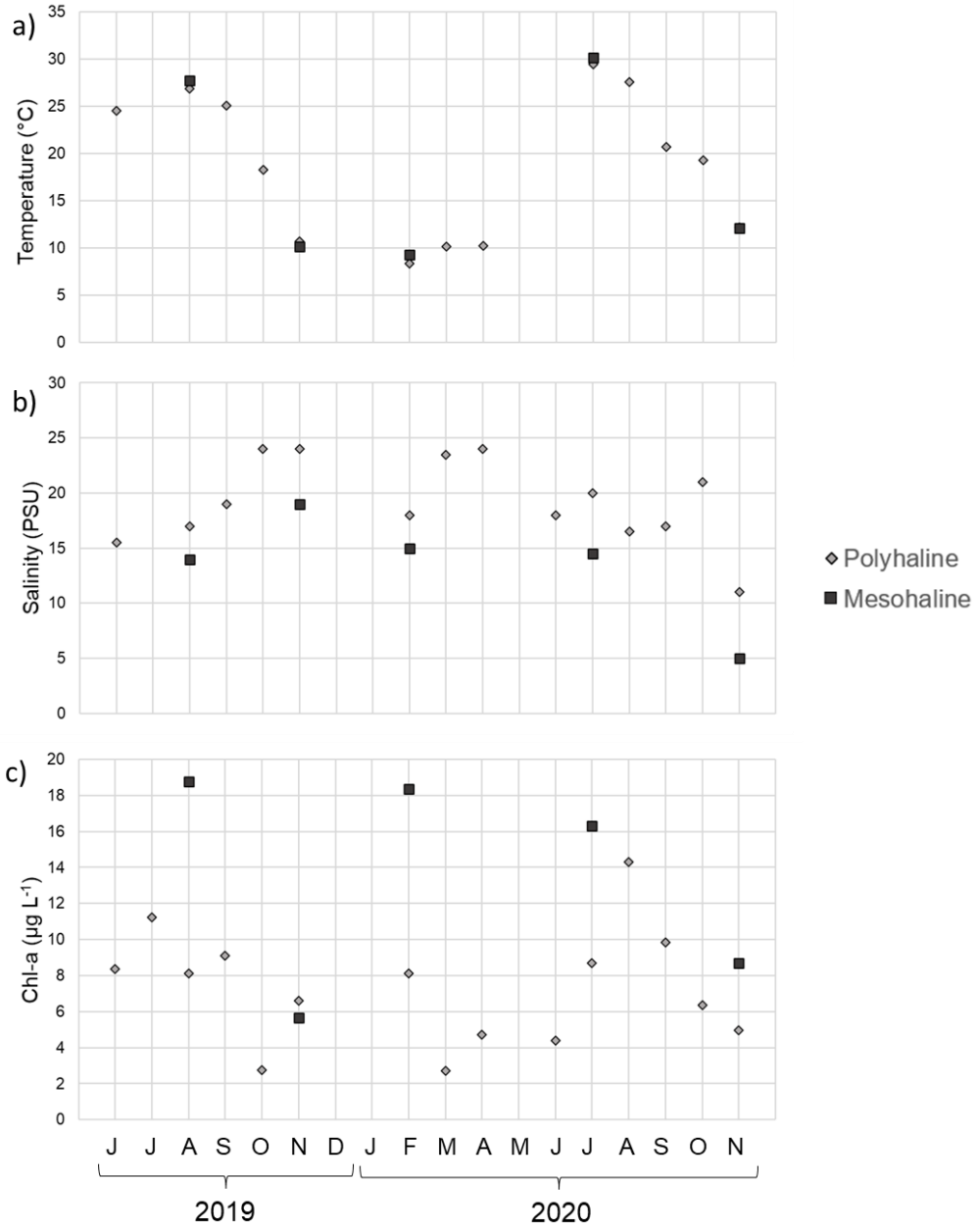

Figure 2. Monthly (a) temperature, (b) salinity, and (c) chlorophyll-a concentrations across the sampling period in the polyhaline and mesohaline sites. Values are average of daytime and nighttime measurements.

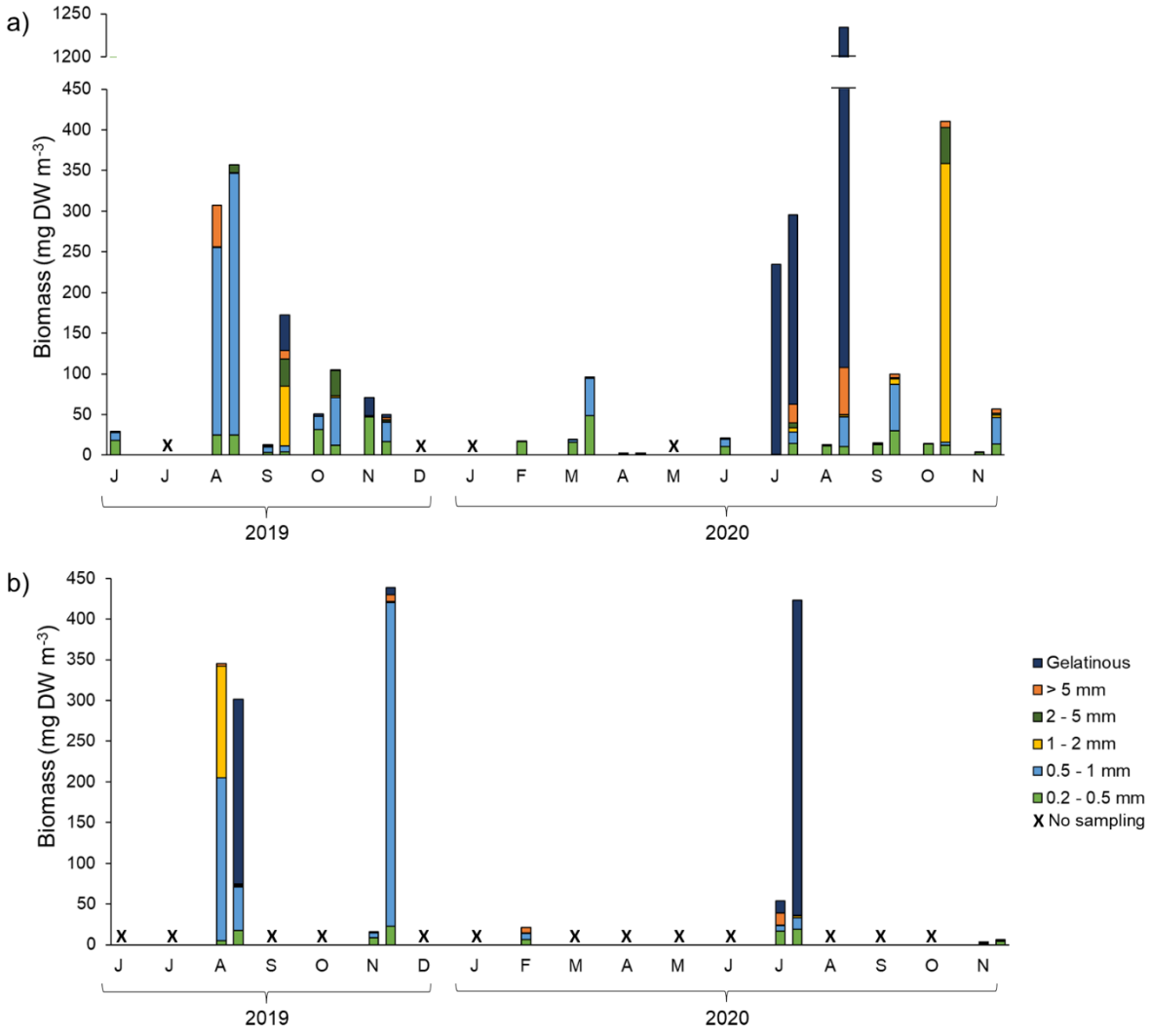

Figure 3. Size-fractionated mesozooplankton biomass in the polyhaline (a) and mesohaline (b) York River. For months with paired day-night tows, the first bar in the pair is day, and the second is night. Only day tows were performed in other months, with X's denoting months in which no sampling occurred. Gelatinous zooplankton (comprised of ctenophores, hydromedusae, and scyphomedusae; see Table 1 and Fig. 7) are shown as a separate category to better illustrate seasonal trends. For all tows n=1.

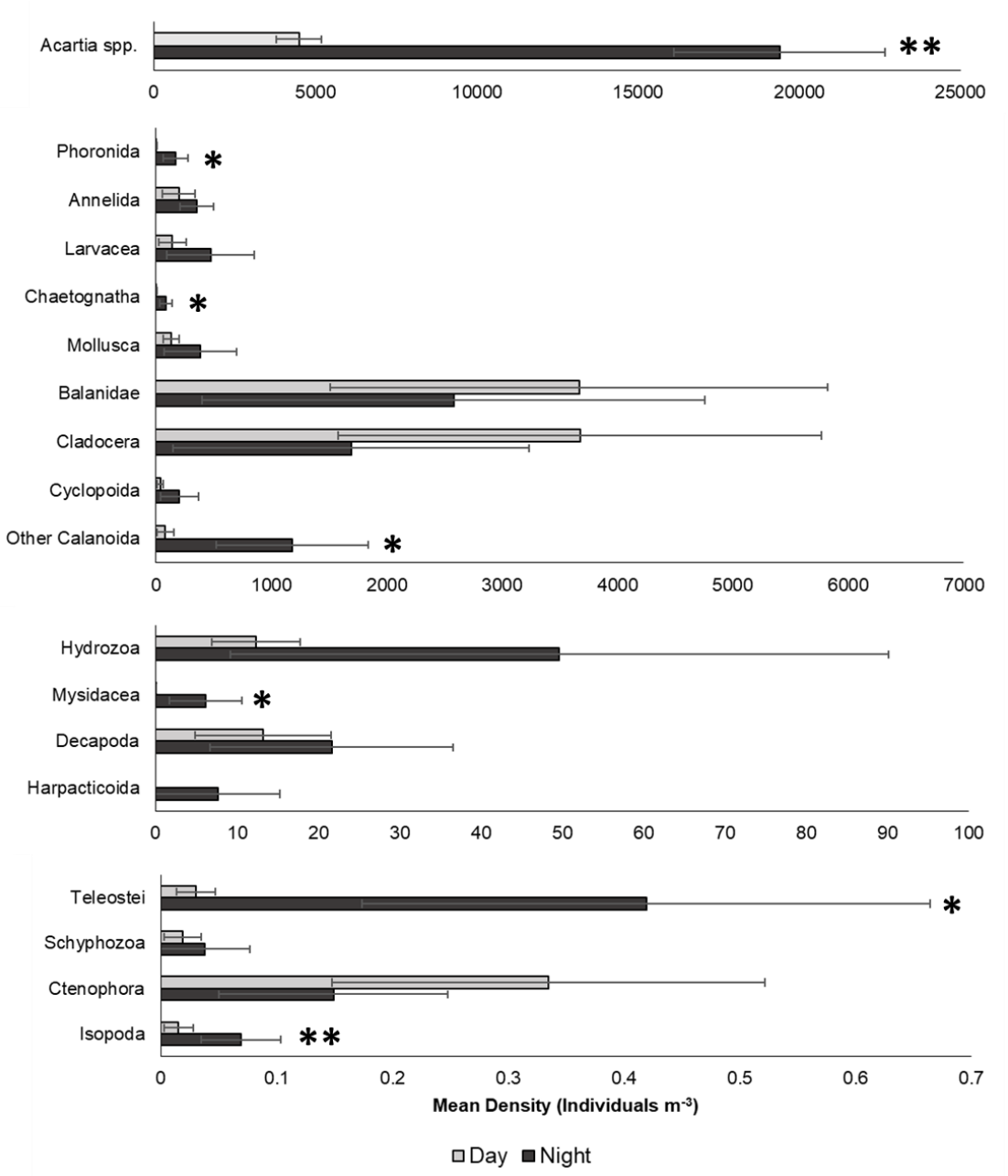

Figure 4. Zooplankton diel vertical migration in the polyhaline York River. Mean day and night (n = 1…5) density of major taxonomic groups in surface waters in the polyhaline sampling site, calculated across the time series (Nov. 2019 to Nov. 2020). Taxa exhibiting diel vertical migration with significantly higher mean densities at night than during the day ($p < 0.05$; student's paired t-test) are marked with two asterisks.

Additional taxa exhibiting strong, but not statistically significant ($0.05 < p < 0.10$) diel vertical migration patterns are marked with one asterisk. See Table 1 for full list and explanation of major taxonomic categories.

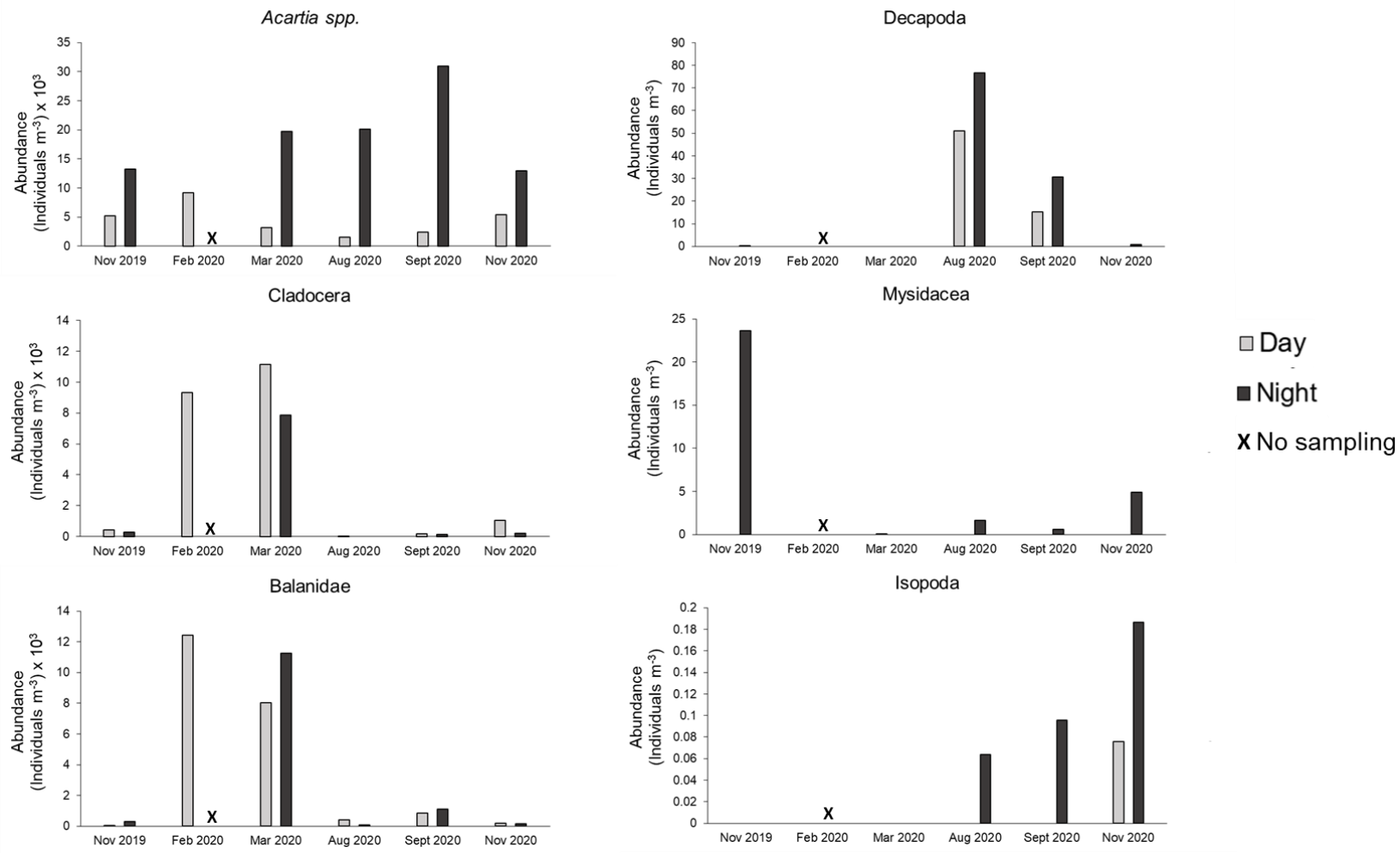
Acartia spp.
Abundance (Individuals m-3) x 10³
Nov 2019
Feb 2020
Mar 2020
Aug 2020
Sept 2020
Nov 2020
Decapoda
Abundance (Individuals m-3)
Cladocera
Mysidacea
Balanidae
Isopoda
Day
Night
x No sampling

Figure 5. Monthly densities of six major taxa of crustaceans in the polyhaline York River during the day and night. The ‘X’ in February 2020 denotes no sampling performed, to distinguish from absence of taxa in other months. See Table 1 for full list and explanation of major taxonomic categories.

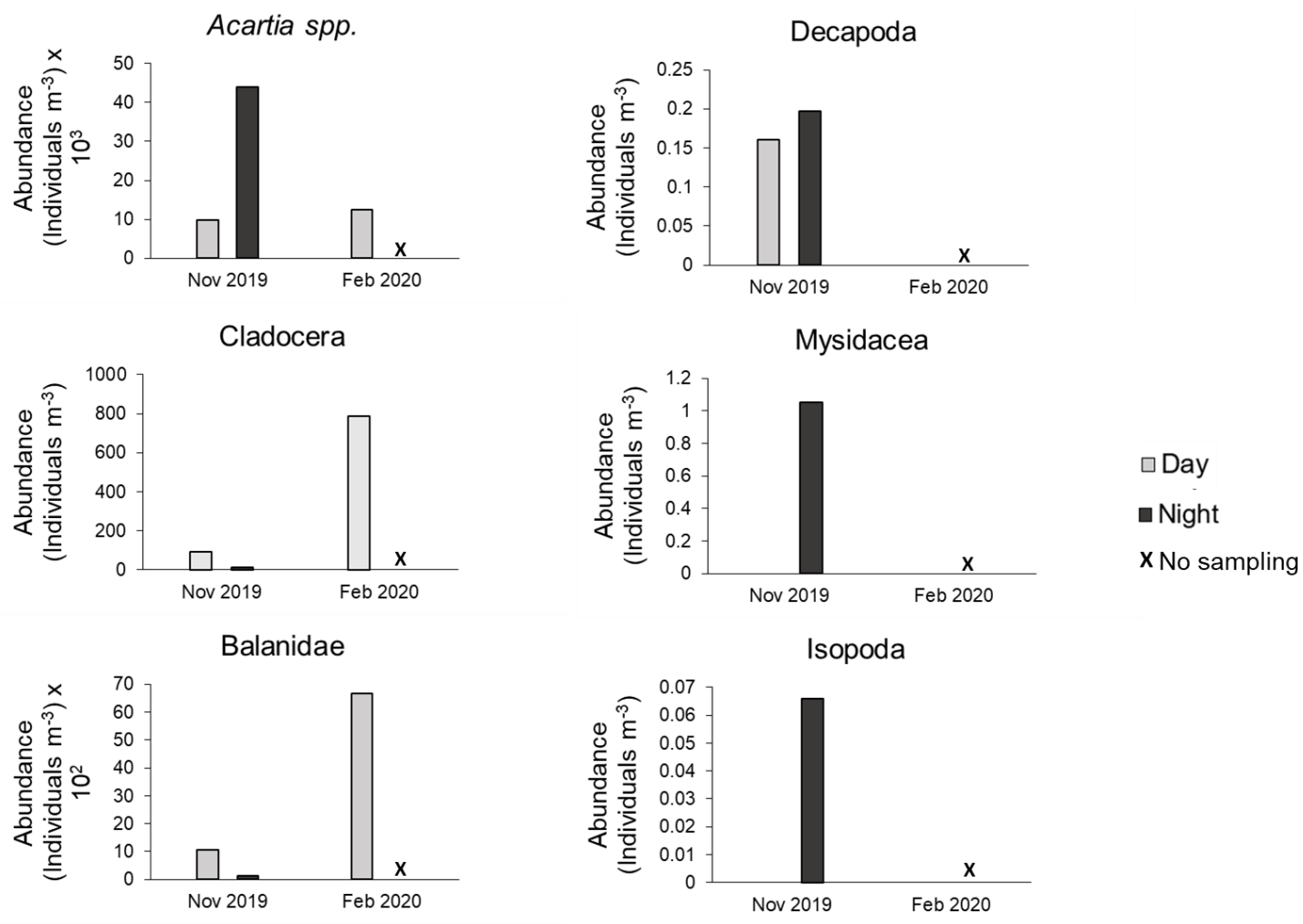
Acartia spp.
Abundance (Individuals m-3) x 10³
50
40
30
20
10
0
X
Nov 2019
Feb 2020
Decapoda
Abundance (Individuals m-3)
0.25
0.2
0.15
0.1
0.05
0
X
Nov 2019
Feb 2020
Cladocera
Abundance (Individuals m-3)
1000
800
600
400
200
0
X
Nov 2019
Feb 2020
Mysidacea
Abundance (Individuals m-3)
1.2
1
0.8
0.6
0.4
0.2
0
X
Nov 2019
Feb 2020
Day
Night
X No sampling
Balanidae
Abundance (Individuals m-3) x 10²
70
60
50
40
30
20
10
0
X
Nov 2019
Feb 2020
Isopoda
Abundance (Individuals m-3)
0.07
0.06
0.05
0.04
0.03
0.02
0.01
0
X
Nov 2019
Feb 2020

Figure 6. Monthly densities of six major taxa of crustaceans in the mesohaline York River during the day and night. The ‘X’ in February 2020 denotes no sampling performed, to distinguish from absence of taxa in other months. See Table 1 for full list and explanation of major taxonomic categories.

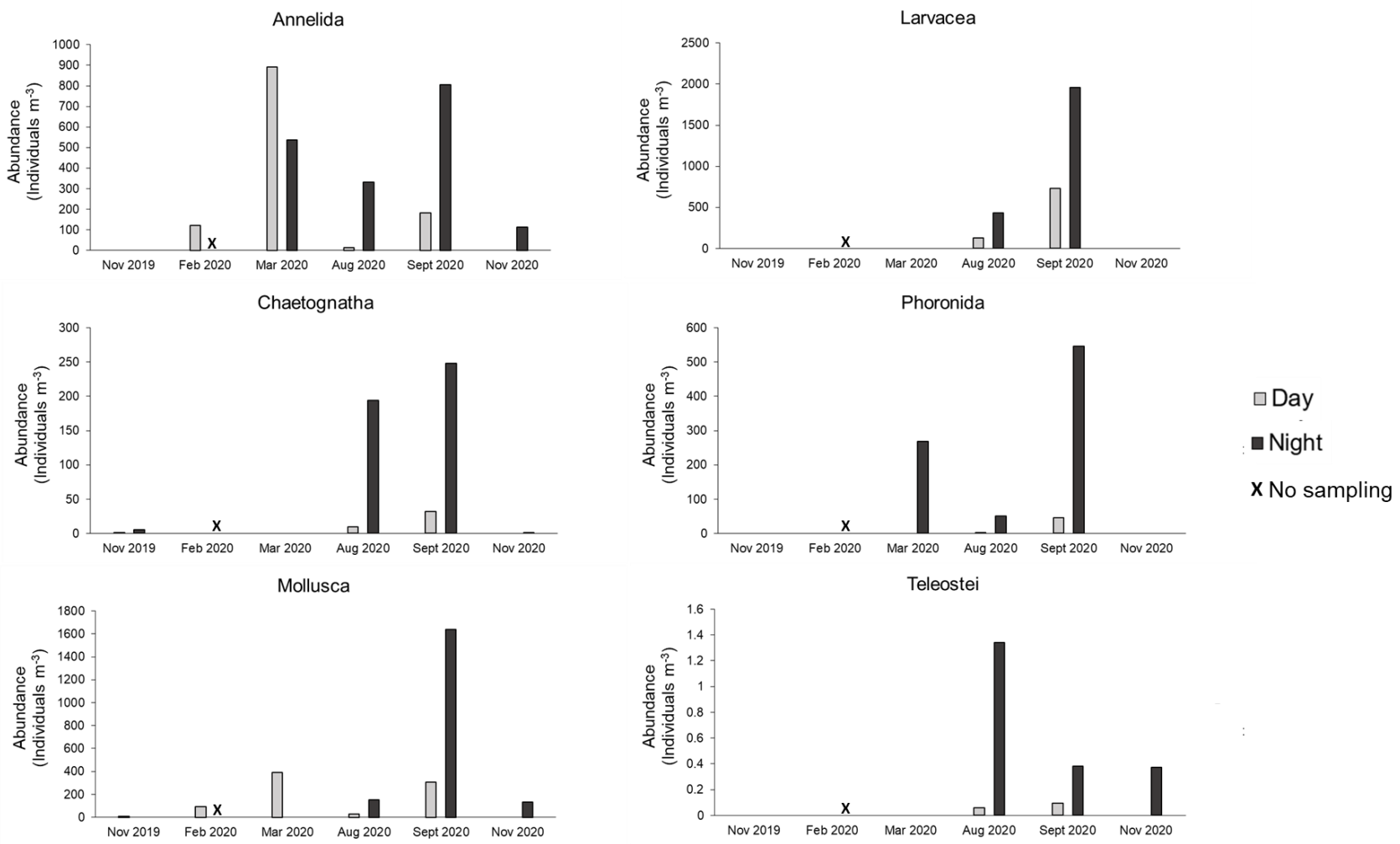
Annelida
Abundance (Individuals m-3)
1000
900
800
700
600
500
400
300
200
100
0
Nov 2019
Feb 2020
Mar 2020
Aug 2020
Sept 2020
Nov 2020
x
Larvacea
Abundance (Individuals m-3)
2500
2000
1500
1000
500
0
Nov 2019
Feb 2020
Mar 2020
Aug 2020
Sept 2020
Nov 2020
x
Chaetognatha
Abundance (Individuals m-3)
300
250
200
150
100
50
0
Nov 2019
Feb 2020
Mar 2020
Aug 2020
Sept 2020
Nov 2020
x
Phoronida
Abundance (Individuals m-3)
600
500
400
300
200
100
0
Nov 2019
Feb 2020
Mar 2020
Aug 2020
Sept 2020
Nov 2020
x
Mollusca
Abundance (Individuals m-3)
1800
1600
1400
1200
1000
800
600
400
200
0
Nov 2019
Feb 2020
Mar 2020
Aug 2020
Sept 2020
Nov 2020
x
Teleostei
Abundance (Individuals m-3)
1.6
1.4
1.2
1
0.8
0.6
0.4
0.2
0
Nov 2019
Feb 2020
Mar 2020
Aug 2020
Sept 2020
Nov 2020
x
Day
Night
x No sampling

Figure 7. Monthly densities of the remaining six major taxa of zooplankton in the polyhaline York River during the day and night. The 'X' in February 2020 denotes no sampling performed, to distinguish from absence of taxa in other months. See Table 1 for full list and explanation of major taxonomic categories.

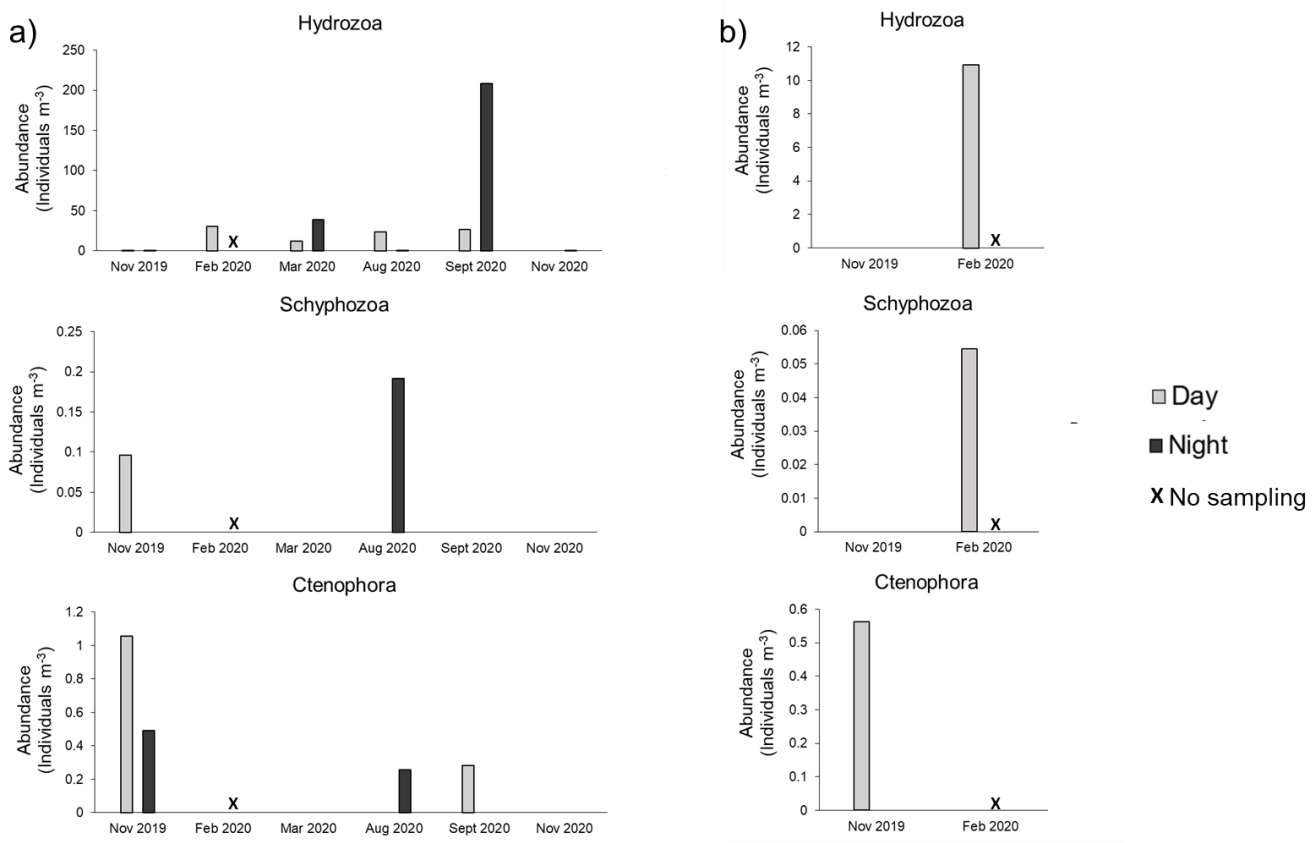

Figure 8. Monthly densities of the three major taxa of gelatinous zooplankton in the (a) polyhaline and (b) mesohaline York River during the day and night. The 'X' in February 2020 denotes no sampling performed, to distinguish from absence of taxa in other months. See Table 1 for full list and explanation of major taxonomic categories.

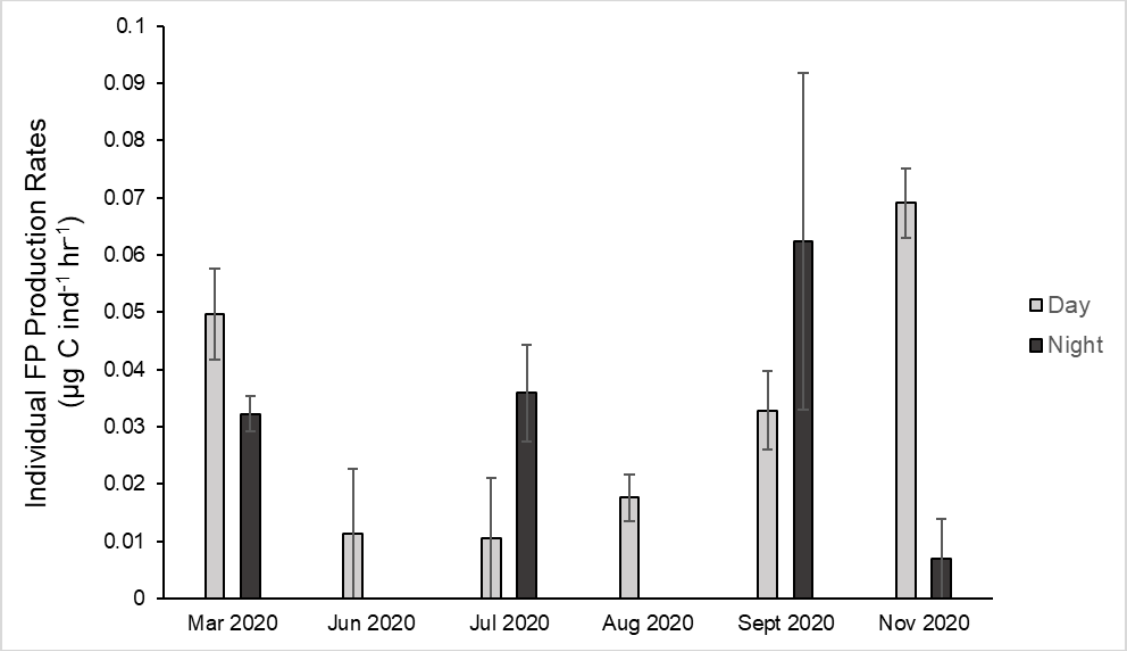

Figure 9. Individual fecal pellet production rates for *Acartia* spp. copepods in the polyhaline York River. Mean rates for daytime (n=6) and nighttime (n=4) experiments are shown; error bars are standard error among replicates within each experiment.

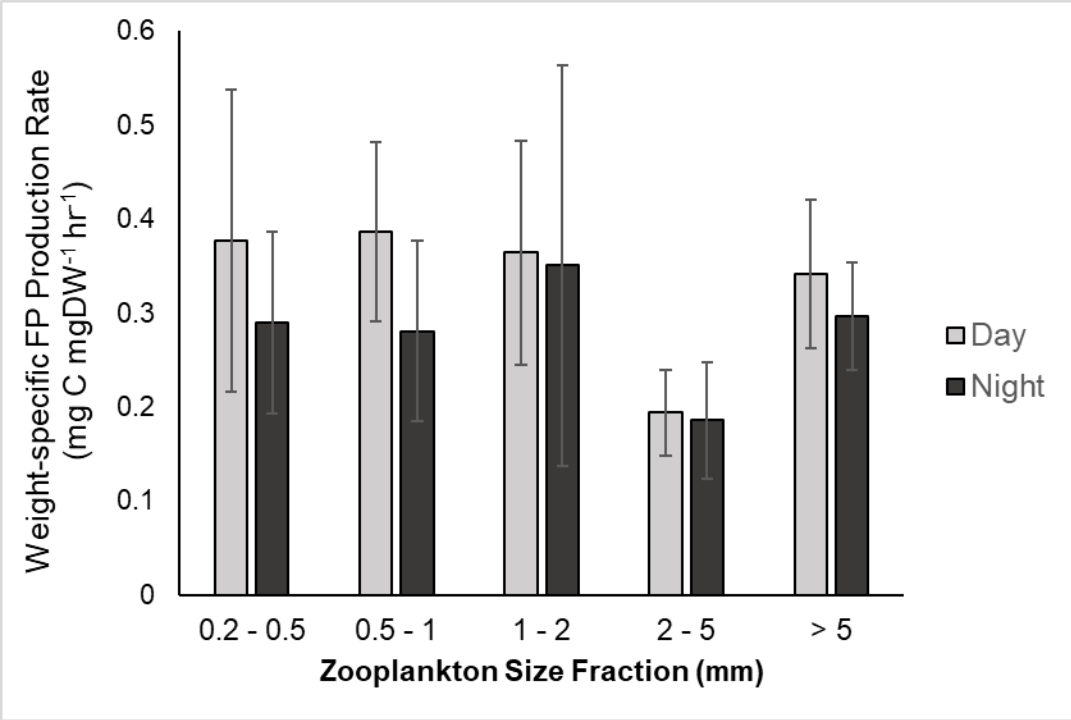

Figure 10. Weight-specific fecal pellet carbon production rates of five mesozooplankton size classes averaged across all experiments in both polyhaline and mesohaline sites in the York River (n=11). Mean rates for daytime and nighttime experiments are shown; error bars are standard error of the means.

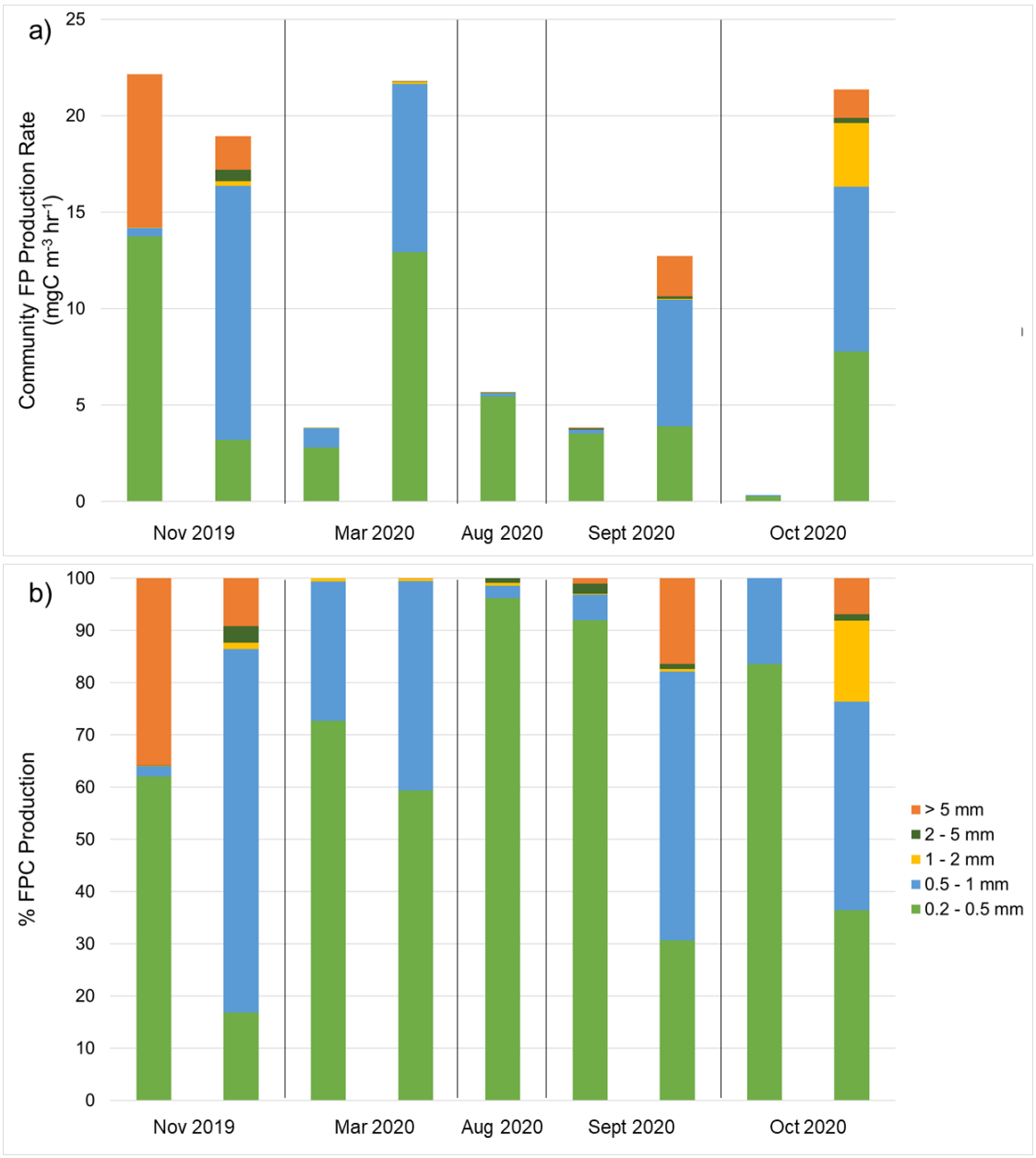

Figure 11. (a) Biomass-corrected (whole community) fecal pellet carbon production rate for five mesozooplankton size classes in the polyhaline York River, and (b) relative (%) contributions of each size class to total community fecal pellet carbon production. Vertical lines separate paired day-night experiments; first bar in the pair is day, and the second is night. Experiment in Aug. 2020 is from the daytime.

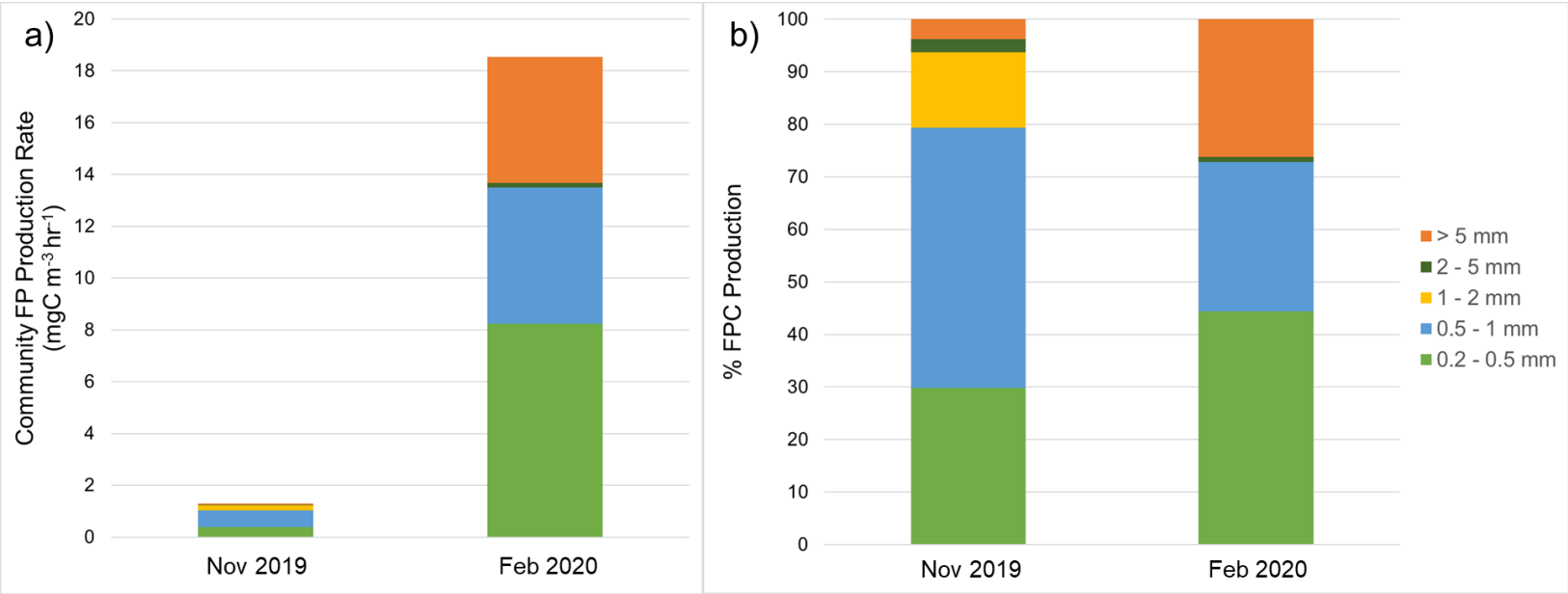

Figure 12. (a) Biomass-corrected (whole community) fecal pellet carbon production rate for five mesozooplankton size classes in the mesohaline York River, and (b) relative (%) contributions of each size class to total community fecal pellet carbon production. Both experiments are during daytime.

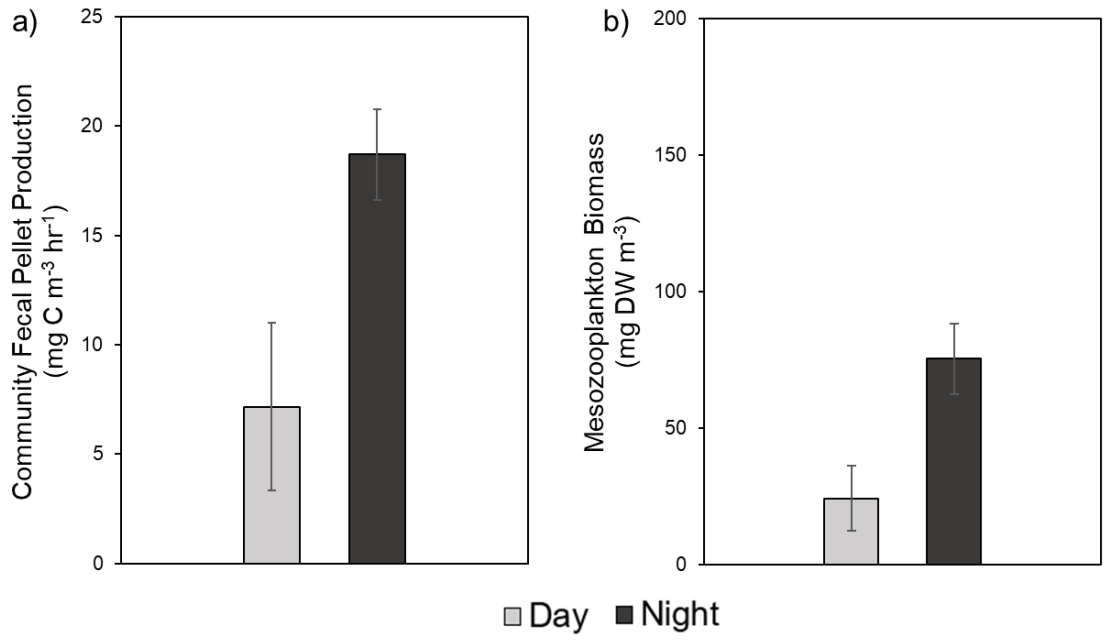

Figure 13. (a) Mean whole-community fecal pellet carbon production rates and (b) mean mesozooplankton biomass in the polyhaline York River, in the day (n=5) versus night (n=4). Error bars are standard error of the means.

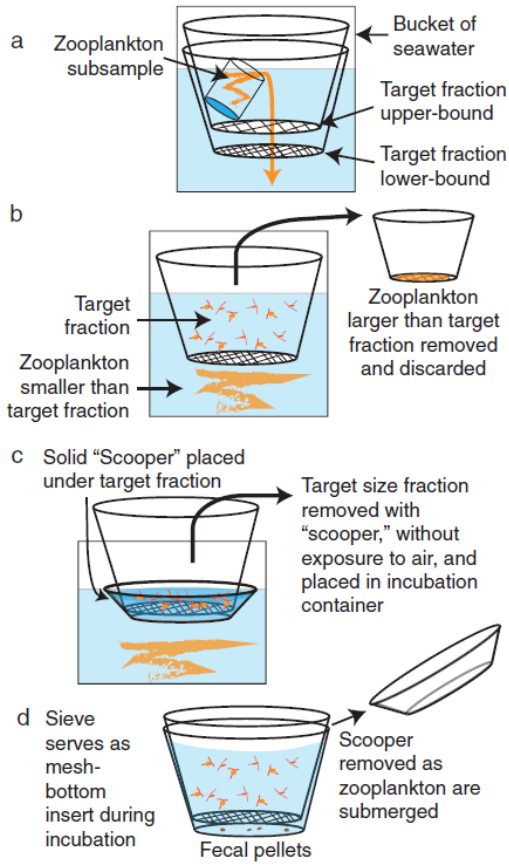

Appendix 1. Schematic from Stamieszkin et al. (2021) showing live size-fractionation methods used in community fecal pellet production experiments. **(a)** Sample is separated into target and non-target fraction using nested sieves. **(b)** Sieves are gently moved in a circular motion and slowly pulled upward to allow zooplankton smaller than the target size fraction to swim out of the bottom mesh. **(c)** A solid "scooper" is used to keep the target zooplankton contained in the mesh-bottomed sieve while also suspended in water. **(d)** The sieve and scooper are placed in the top of the experimental container full of whole seawater, the scooper is gently removed, and the nested sieve is slowly lowered into the container, covered with a lid, and incubated at ambient temperature and light conditions.

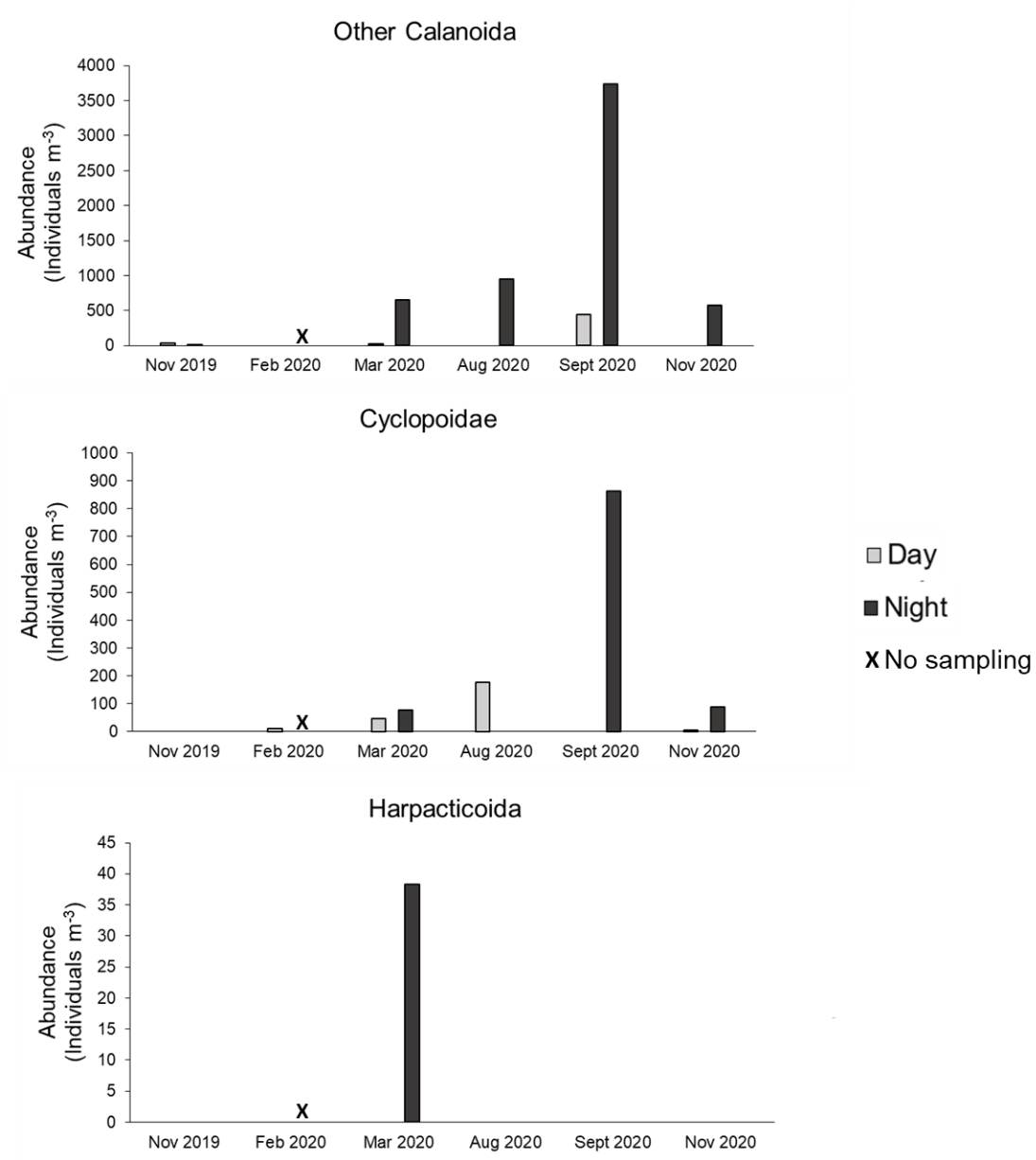

Appendix 2. Monthly densities of three major taxa of non-*Acartia* copepods in the polyhaline York River during the day and night. The 'X' in February 2020 denotes no sampling performed, to distinguish from absence of taxa in other months. See Table 1 for full list and explanation of major taxonomic categories.

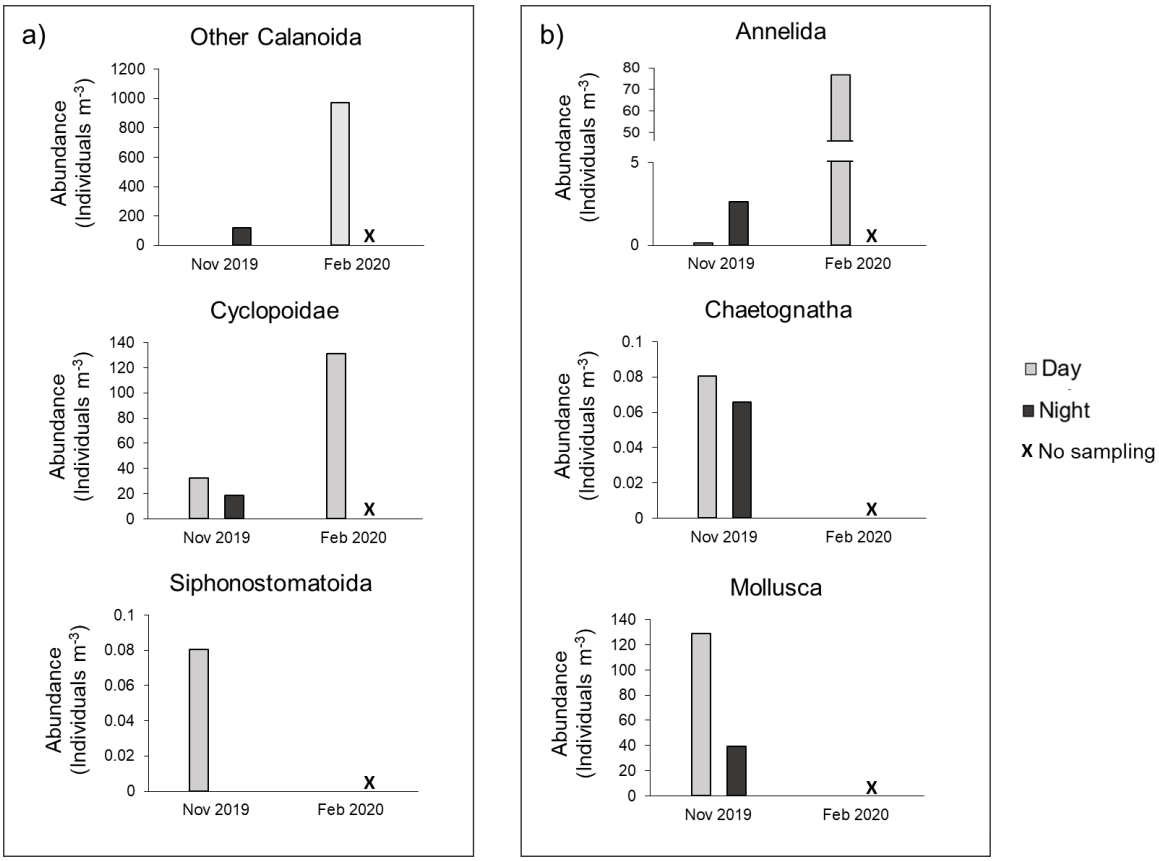

Appendix 3. Monthly densities of the (a) three major taxa of non-*Acartia* copepods and (b) remaining three major taxa of mesozooplankton in the mesohaline York River during the day and night. The 'X' in February 2020 denotes no sampling performed, to distinguish from absence of taxa in other months. See Table 1 for full list and explanation of major taxonomic categories.

VITA

KRISTEN NICOLE SHARPE

Born in Rome, NY. Received a Bachelor of Science degree in Biological Applications of Environmental Studies from the SUNY College of Environmental Science & Forestry and Syracuse University in May 2013. Awarded top scholar within the Environmental Studies major at Convocation. Employed as a marine science educator at the Chesapeake Bay National Estuarine Research Reserve in Virginia from January 2014 to August 2018, working with thousands of students and members of the public. Served as Vice-President of the Three Rivers Environmental Educators workgroup, and Virginia State Representative and Social Media Chair of the Mid-Atlantic Marine Education Association. Entered the VIMS Master of Science program in August 2018 under advisor Dr. Deborah Steinberg. Elected First Year Representative on the VIMS Graduate Student Association (GSA) executive board in 2018-2019 and was awarded the Kelley Watson Memorial Fellowship for first-year student academic achievement in 2019. Elected Co-President of the GSA from 2019-2021. Served as Climate Science Lead for the National Network of Ocean and Climate Change Interpretation's Hampton Roads Study Circle in 2019. Participated in the Western Antarctic Peninsula PAL LTER research cruise in winter 2020 and the NASA EXPORTS Northeast Atlantic research cruise in spring 2021. Awarded the Beazley Fellowship for academic achievement and merit in 2020. Named a William & Mary Woman of Influence for the 2020-2021 academic year.